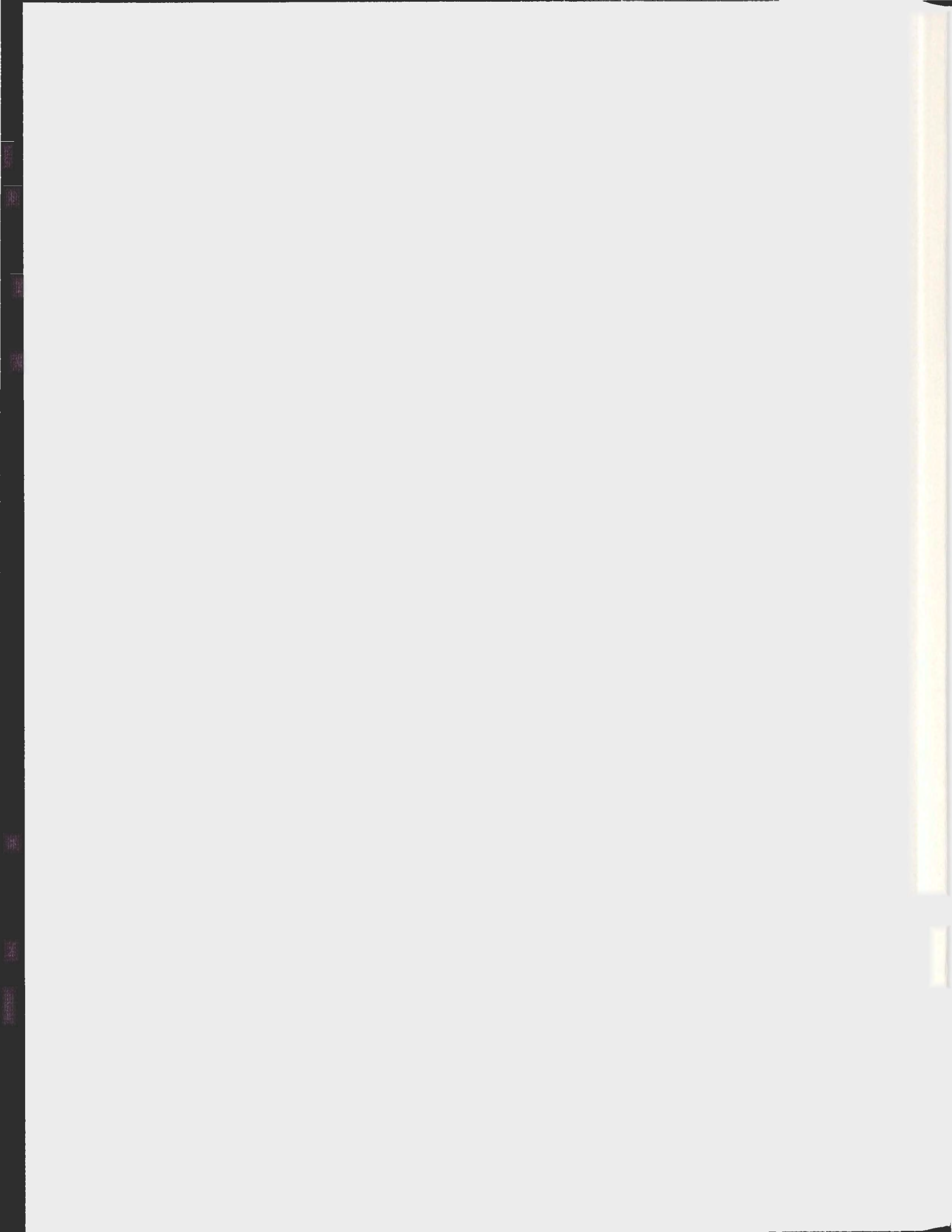


TRAVELING WAVEFRONTS OF NON-LOCAL
REACTION-DIFFUSION MODELS FOR CELL
ADHESION AND CANCER INVASION

YI ZHANG



**Traveling Wavefronts of Non-local
Reaction-diffusion Models for Cell Adhesion and
Cancer Invasion**

by

©Yi Zhang

A (Thesis, Dissertation, or Report) submitted to the School of Graduate Studies in
partial fulfillment of the requirements for the degree of

Master of Science

Department of Mathematics and Statistics

Memorial University of Newfoundland

August, 2012

St. John's

Newfoundland

Abstract

Cell adhesion is a fundamental mechanism binding a cell to a surface, extracellular matrix or another cell through cell adhesion molecules. This cell behavior is involved in various biological processes including embryogenesis, migration and invasion, tissue remodeling and wound healing. This paper investigates the existence of traveling wavefronts of a non-local reaction-diffusion model for cell behavior proposed first by Armstrong *et al.* (J. Theor. Biol., 243 (2006), 98-113), and by Sherratt *et al.* (European J. Appl. Math., 20 (2009), 123-144). We provide a valid approach by using perturbation methods and the Banach fixed point theorem to show the existence of wavefronts for the model with some suitable parameter values. Numerically, the solutions with initial step functions eventually stabilize to a smooth wavefront for a relatively small adhesion coefficient. We also consider the application of this model to study the cancer invasion process, which results in a system with solutions reflecting the relation between cell-cell and cell-matrix adhesion in the cancer invasion regulation. Using the same method employed in the cell-adhesion model, the existence of traveling wavefronts to this system is established. Finally numerical simulations are presented to verify the effectiveness of our proposed theoretical results and to demonstrate some new phenomena that deserve further study in the future.

Acknowledgements

I would like to express my grateful and sincere thank to Dr. Chunhua Ou for his patient guidance and ceaseless refinements. I also thank the referees for agreeing to read this thesis, from whom any suggestions or comments are valuable. Finally, I would like to thank the department administrators, Ros English, Leonce Morrissey, and Dr. JC Loreda Osti, for their patience and courtesy in answering my emails.

Table of Contents

Abstract	ii
Acknowledgments	iii
Table of Contents	vi
List of Figures	x
1 Introduction	1
1.1 Cell adhesion and cancer invasion	1
1.2 Previous modeling work	2
1.3 Outline	3
2 Mathematical model for cell adhesion	5
2.1 Introduction of the cell adhesion model	5
2.2 Description of notation	6
2.3 Dimensionless model for cell adhesion	8
3 Existence of wave patterns for small α	10
3.1 Critical wave speed	10
3.2 Traveling wave solutions for $\alpha = 0$	12
3.3 Traveling wave solutions for α sufficiently small	13

3.3.1	Notations of spaces and norms	13
3.3.2	Approximation of wavefronts by using perturbation methods .	14
3.3.3	Demonstration of the existence of traveling waves for small α .	16
3.3.3.1	Approximation of $R(V)$ and $Q(z, V)$	17
3.3.3.2	Surjective mapping L	19
3.3.3.3	The main theorem	22
4	Application to cancer invasion	25
4.1	Introduction of the cancer invasion model	25
4.2	Description of notation	27
4.3	Dimensionless model for cancer invasion	28
5	Wave solutions of the system (4.4) for small χ	30
5.1	Traveling wave solutions for the limiting system when $\chi = 0$	31
5.2	Traveling wave solutions for χ sufficiently small	32
5.2.1	Approximation of wavefronts by using perturbation methods .	33
5.2.2	Demonstration of the existence of traveling waves for small χ .	36
5.2.2.1	Approximation of $R_1(W_1)$ and $Q_1(z, W_1)$	37
5.2.2.2	The main theorem	39
6	Simulations	43
6.1	Traveling waves of the cell adhesion model for small α	44
6.1.1	The finite difference scheme of the cell adhesion model	44
6.1.2	Numerical results and figures	48
6.1.3	A second numerical approach	48
6.1.3.1	Approximation of $S(n(x, t))$	52
6.1.3.2	Numerical results	54
6.2	Traveling waves of the cancer invasion model for small χ	54

6.2.1	The finite difference scheme of the cancer invasion model . . .	56
6.2.2	Numerical figures and results	58
6.2.3	A second numerical approach	59
6.2.3.1	Approximation of $K(n(x,t), m(x,t))$	66
6.2.3.2	Numerical results	67
6.2.4	An alternate initial function for matrix distribution	67
7	Discussion	75
	Bibliography	77

List of Figures

6.1	Numerical solutions of the model (6.1) with $\alpha = 0.1$. Traveling wave solutions of cell density $n(x, t)$ for time period $t \in [0, 10]$ with the initial conditions (6.6) and $\alpha = 0.1$	49
6.2	Numerical solutions of the model (6.1) with $\alpha = 0.1$. Traveling wave solutions of cell density $n(x, t)$ at different time points for $\alpha = 0.1$	49
6.3	Numerical solutions of the model (6.1) with $\alpha = 1$. Traveling wave solutions of cell density $n(x, t)$ for time period $t \in [0, 10]$ with the initial conditions (6.6) and $\alpha = 1$	50
6.4	Numerical solutions of the model (6.1) with $\alpha = 1$. Traveling wave solutions of cell density $n(x, t)$ at different time points for $\alpha = 1$	50
6.5	Numerical solutions of the model (6.1) with $\alpha = 2$. Traveling wave solutions of cell density $n(x, t)$ for time period $t \in [0, 10]$ with the initial conditions (6.6) and $\alpha = 2$	51
6.6	Numerical solutions of the model (6.1) with $\alpha = 2$. Traveling wave solutions of cell density $n(x, t)$ at different time points for $\alpha = 2$	51
6.7	Numerical solutions of the model (6.1) with $\alpha = 3$. Traveling wave solutions of cell density $n(x, t)$ for time period $t \in [0, 20]$ with the initial conditions (6.6) and $\alpha = 3$	55

6.8	Numerical solutions of the model (6.1) with $\alpha = 5$. Traveling wave solutions of cell density $n(x, t)$ for time period $t \in [0, 20]$ with the initial conditions (6.6) and $\alpha = 5$	55
6.9	Numerical solutions of system (6.14) for $\chi = 1$. Traveling wave solutions of the tumor cell density $n(x, t)$	59
6.10	Numerical solutions of system (6.14) for $\chi = 1$. Traveling wave solutions of the extracellular matrix density $m(x, t)$	60
6.11	Numerical solutions of system (6.14) for $\chi = 1$. Wavefronts of the tumor cell density $n(x, t)$ at different time points for $t \in [0, 10]$	60
6.12	Numerical solutions of system (6.14) for $\chi = 1$. Wavefronts of the extracellular matrix density $m(x, t)$ at different time points for $t \in [0, 10]$	61
6.13	Numerical solutions of system (6.14) for $\chi = 6$. Traveling wave solutions of the tumor cell density $n(x, t)$	61
6.14	Numerical solutions of system (6.14) for $\chi = 6$. Traveling wave solutions of the extracellular matrix density $m(x, t)$	62
6.15	Numerical solutions of system (6.14) for $\chi = 6$. Wavefronts of the tumor cell density $n(x, t)$ at different time points in the beginning for $t \in [0, 1]$	62
6.16	Numerical solutions of system (6.14) for $\chi = 6$. Wavefronts of the extracellular matrix density $m(x, t)$ at different time points for $t \in [0, 10]$	63
6.17	Numerical solutions of system (6.14) for $\chi = 25$. Traveling wave solutions of the tumor cell density $n(x, t)$	63
6.18	Numerical solutions of system (6.14) for $\chi = 25$. Traveling wave solutions of the extracellular matrix density $m(x, t)$	64
6.19	Numerical solutions of system (6.14) for $\chi = 25$. Wavefronts of the tumor cell density $n(x, t)$ at different time points in the beginning for $t \in [0, 1]$	64

6.20	Numerical solutions of system (6.14) for $\chi = 25$. Wavefronts of the extracellular matrix density $m(x, t)$ at different time points for $t \in [0, 10]$	65
6.21	Numerical solutions of system (6.14) for $\chi = 7$. These are the solution figures of tumor cell density $n(x, t)$ (upper wave) and extracellular matrix density $m(x, t)$ (lower wave) for time period $t \in [0, 30]$ with the adhesion coefficient $\chi = 7$	68
6.22	Numerical solutions of system (6.14) for $\chi = 7$. Wavefronts of the tumor cell density $n(x, t)$ at different time points.	68
6.23	Numerical solutions of system (6.14) for $\chi = 7$. Wavefronts of the extracellular matrix density $m(x, t)$ at different time points.	69
6.24	Numerical solutions of system (6.14) for $\chi = 1$. These are the solution figures of tumor cell density $n(x, t)$ (upper wave) and extracellular matrix density $m(x, t)$ (lower wave) with the adhesion coefficient $\chi = 1$	70
6.25	Numerical solutions of system (6.14) for $\chi = 1$. Wavefronts of the tumor cell density $n(x, t)$ at different time points.	70
6.26	Numerical solutions of system (6.14) for $\chi = 1$. Wavefronts of the extracellular matrix density $m(x, t)$ at different time points.	71
6.27	Numerical solutions of system (6.14) for $\chi = 4$. These are the solution figures of tumor cell density $n(x, t)$ (upper wave) and extracellular matrix density $m(x, t)$ (lower wave) with the adhesion coefficient $\chi = 4$	71
6.28	Numerical solutions of system (6.14) for $\chi = 4$. Wavefronts of the tumor cell density $n(x, t)$ at different time points.	72
6.29	Numerical solutions of system (6.14) for $\chi = 4$. Wavefronts of the extracellular matrix density $m(x, t)$ at different time points.	72

6.30	Numerical solutions of system (6.14) for $\chi = 6$. These are the solution figures of tumor cell density $n(x, t)$ (upper wave) and extracellular matrix density $m(x, t)$ (lower wave) with the adhesion coefficient $\chi = 6$	73
6.31	Numerical solutions of system (6.14) for $\chi = 6$. Wavefronts of the tumor cell density $n(x, t)$ at different time points.	73
6.32	Numerical solutions of system (6.14) for $\chi = 6$. Wavefronts of the extracellular matrix density $m(x, t)$ at different time points.	74

Chapter 1

Introduction

1.1 Cell adhesion and cancer invasion

Adhesion of cells is an important biological regulator that describes the binding of one cell to another and to their environment through cell surface proteins known as cell-adhesion molecules (CAMs). This process plays a key role in tissue homeostasis, embryo development and tumor growth; see [4, 24]. Foty and Steinberg [16] proposed a differential adhesion hypothesis and correctly predicted the experimental results on cell adhesion and tissue rearrangements. For more recent research in this area, see also Reddig and Juliano [36].

As a general phenomenon in biological environments, cell adhesion has a strong influence on the cellular invasion process in cancer, where cancer cells break out of tissue compartments and spread into the surrounding extracellular matrix. It plays a key role in the metastatic cascade, where tumor cells leave the original tumor site and spread via the bloodstream or the lymphatic system into a distinct organ or part of the body; see [20, 25]. Solid tumor cells create excessive proteolytic enzymes, such as the urokinase-type plasminogen activator (uPA) and matrix metalloproteinases

(MMPs), in the early stages of invasion. See [13, 14, 15, 39] for a discussion of the growth of solid tumor cells. With these enzymes, the surrounding extracellular matrix degrades, which enables the proliferation of cancer cells and separates tumors from the adjoining tissue. By the degradation of the matrix, cancer cells are able to breach the extracellular matrix and escape to a secondary site in the body.

1.2 Previous modeling work

Based on the assumption that cells move in response to chemotactic and/or haptotactic cues, a large number of mathematical models of cancer cell invasion have been studied to explore the diverse aspects of tumor growth dynamics. For example, in Anderson *et al.* [2], Araujo and McElwain [3], Chaplain and Lolas [6, 7], Gatenby [21], Gatenby and Gawlinski [22], all of them use continuum model systems of partial differential equations. Meanwhile, a discrete approach based on individual cell identity has also been adopted, where significant attention has been paid to cell-cell adhesion; see [1, 2, 11, 38]. With a combination of both continuum and discrete approaches, the hybrid modeling technique has been applied to studying patterns of cancer invasion by Anderson [1], Dorman and Deutsch [10], Ignacio *et al.* [27], Jeon *et al.* [28].

Most of the early continuum models of cancer invasion neglect to consider the effect of cell-cell adhesion. A recent effective approach to the problem of cell adhesion involves the incorporation of adhesion via a surface tension of the tumor boundary. See Byrne and Chaplain [5], Chaplain [8], Cristini *et al.* [9], Frieboes *et al.* [17] and [18], Friedman [19], Macklin and Lowengrub [29] for more details. Armstrong *et al.* [4] have developed a continuum model for cell motility due to cell-cell adhesion, where the non-local interaction term was described by an integro-partial differential equation. They extended the model for interactions between multiple populations

and discussed the cell adhesion model in both 1-D and 2-D; see also Hillen [26]. However, these approaches did not investigate the cell-matrix adhesion, which has been demonstrated to play an important role in the invasion process.

Based on the work of Armstrong *et al.* [4], some continuum models for cancer invasion have recently been further investigated via an integro-partial differential equation, incorporating the adhesion effects of both cell-cell and cell-matrix; see Gerisch and Chaplain [23], Painter *et al.* [34], Sherratt *et al.* [37]. On a bounded domain, Sherratt *et al.* [37] formulated a non-local reaction-diffusion model for cell adhesion in cell aggregation and also applied the model to cancer invasion, where the non-local term reflected the balance between cell-cell and cell-matrix adhesion in regulating cancer invasion. The authors also derived several conditions which were sufficient for the boundedness of the solutions and investigated the effect of adhesion on cell aggregation and cancer invasion by numerical simulations. Similar numerical results were also provided by Painter *et al.* [34]. The above researchers have simulated and observed the cell aggregation and cancer cell invasion with the patterns of wavefronts. However, to the best of our knowledge, no rigorous work has previously been done for the existence of traveling wave solutions in such continuum models.

1.3 Outline

This thesis begins in chapter 2 by presenting the non-local continuum model for cell adhesion, proposed, for example, by Sherratt *et al.* [37], where the non-local term is given by an integro-partial differential equation. Using the Banach fixed point theorem, chapter 3 illustrates the existence of traveling wavefronts of the cell adhesion model with relatively small adhesion coefficient. The whole proof is based on perturbation methods, where the solution of the model closely relates to the one of

the limiting model with zero adhesion coefficient (no adhesion). For similar methods, see [32] and [33]. Chapter 4 considers the cancer invasion model in [37] including both cell-cell and cell-matrix adhesion, which is in fact an important application and extension of the simple cell-adhesion model. The existence of traveling wave solutions of this cancer invasion model is demonstrated in chapter 5 using the same approach as considered in chapter 3. Chapter 6 provides numerical simulations to verify the main results. Conclusions and some suggestions of future work are discussed in chapter 7.

Chapter 2

Mathematical model for cell adhesion

This chapter re-visits the non-local reaction-diffusion model for cell adhesion, which includes three kinds of cell behaviors: diffusion, adhesion, and cell kinetics. The model is based on the work of Armstrong *et al.* [4] and Sherratt *et al.* [37], which illustrates the formation of cell aggregation by sufficiently strong cell-cell adhesion from an initially randomly distributed population of cells on a bounded domain.

2.1 Introduction of the cell adhesion model

For mathematical simplicity, this section considers the movement of a single cell population with uniform adhesive properties in one space dimension and investigates the mathematical model for cell-cell adhesion. Considering the forces acting on the cells in a conservative system, the continuum mathematical model of cell adhesion is given by

$$\frac{\partial n(x, t)}{\partial t} = \overbrace{D \frac{\partial^2 n(x, t)}{\partial x^2}}^{\text{Diffusion}} - \overbrace{\frac{\partial}{\partial x} [n(x, t) S(n(x, t))]}^{\text{Adhesion}} + \overbrace{f(n)}^{\text{Cell kinetics}}, \quad (2.1)$$

where $n(x, t)$ is the cell density at time t and position x , and

$$S(n(x, t)) = \frac{\alpha\phi}{R} \int_{-R}^R A(n(x + x_0, t))\omega(x_0)dx_0. \quad (2.2)$$

$S(n(x, t))$ is the non-local adhesion term which describes the total forces acting on the cells. For more detail about the model derivation, see [4]. Therefore, with the substitution of (2.2) into (2.1), the model is established by the integro-partial differential equation

$$\begin{aligned} \frac{\partial n(x, t)}{\partial t} = D \frac{\partial^2 n(x, t)}{\partial x^2} + f(n) \\ - \frac{\alpha\phi}{R} \frac{\partial}{\partial x} \left[n(x, t) \int_{-R}^R A(n(x + x_0, t))\omega(x_0)dx_0 \right], \end{aligned} \quad (2.3)$$

where the effect of cell-cell adhesion is reflected through the partial derivative of an integral over the sensing region of a cell. From the description in [4] and [37], $D > 0$ is the diffusion coefficient. α , ϕ , R are positive parameters relating to cell adhesion, where α is the adhesion coefficient, ϕ represents the cell-viscosity, and R is the sensing radius of cells over which cells can sense their surroundings.

2.2 Description of notation

In (2.3), the integral describes the total attracting force acting on the cells. Specifically, $A(n(x + x_0, t))$ represents the local adhesive forces created by cells at position x with cells a distance x_0 away, where the sensing radius R is the maximum of $|x_0|$. With the dependence on the local cell density, the local adhesion forces of cells will increase with the cell density below a threshold density and eventually decrease. The

logistic type function was used in [4] and [37] for $A(n)$:

$$A(n(x + x_0, t)) = \begin{cases} n(x + x_0, t)(1 - n(x + x_0, t)/n_{max}), & n(x + x_0, t) < n_{max}, \\ 0, & \text{otherwise,} \end{cases} \quad (2.4)$$

where n_{max} is the carrying capacity of the cell population. Equivalently, $A(n) = \max\{n(1 - n/n_{max}), 0\}$ is the local adhesive force function for mathematical simplicity. See [4] and [37] for more details.

The function $\omega(x_0)$ represents the variation of the direction and magnitude of the adhesive force over the sensing region of the cell. Due to the “pulling” nature, the adhesive force is always directed towards cell centers. Following Armstrong *et al.* [4] and Sherratt *et al.* [37], we choose $\omega(x_0) = (1/R) \text{sign}(x_0)$ on $x_0 \in [-R, R]$ such that $\omega(x_0)$ is an odd function satisfying the condition $\int_0^R \omega(x_0) dx_0 = 1$. Therefore, the total adhesive force on cells denoted by the integral in (2.3) is the sum of local forces given by $A(n)$ and $\omega(x_0)$.

As for the cell kinetics, Sherratt *et al.* [37] use the logistic function: $f(n) = \mu n(1 - n/n_0)$, where μ is the growth rate, and $n_0 < n_{max}$ is the critical value above which the new generation of cells by division becomes slower than cell loss.

2.3 Dimensionless model for cell adhesion

From the above description, the non-local reaction-diffusion model (2.3) for cell adhesion is given by

$$\begin{aligned} \frac{\partial n(x,t)}{\partial t} = & D \frac{\partial^2 n(x,t)}{\partial x^2} + \mu n \left(1 - \frac{n}{n_0}\right) \\ & - \frac{\alpha \phi}{R^2} \frac{\partial}{\partial x} \left[n(x,t) \int_{-R}^R \max \left\{ n(x+x_0,t) \left(1 - \frac{n(x+x_0,t)}{n_{max}}\right), 0 \right\} \right. \\ & \left. \cdot \text{sign}(x_0) dx_0 \right]. \end{aligned} \tag{2.5}$$

To non-dimensionalize equation (2.5), let

$$x^* = \frac{x}{R}, \quad x_0^* = \frac{x_0}{R}, \quad D^* = \frac{D}{R^2}, \quad n^* = \frac{2n}{n_{max}}, \quad \alpha^* = \frac{\alpha \phi n_{max}}{4R^2}, \quad n_0^* = \frac{2n_0}{n_{max}}.$$

Dropping the asterisks for simplicity, a dimensionless model of cell adhesion on $x \in (-\infty, +\infty)$ is given by

$$\begin{aligned} \frac{\partial n(x,t)}{\partial t} = & D \frac{\partial^2 n(x,t)}{\partial x^2} - \frac{\partial}{\partial x} [n(x,t)S(n(x,t))] + f(n) \\ = & D \frac{\partial^2 n(x,t)}{\partial x^2} - \alpha \frac{\partial}{\partial x} \left[n(x,t) \int_{-1}^{+1} A(n(x+x_0,t)) \omega(x_0) dx_0 \right] \\ & + \mu n \left(1 - \frac{n}{n_0}\right), \end{aligned} \tag{2.6}$$

where the total cell-adhesion forces become

$$S(n(x,t)) = \alpha \int_{-1}^1 A(n(x+x_0,t)) \omega(x_0) dx_0, \tag{2.7}$$

and $A(n(x+x_0, t)) = \max\{n(x+x_0, t)[2-n(x+x_0, t)], 0\}$ is the rescaled version of the local force function and $\omega(x_0) = \text{sign}(x_0)$. Specifically, α is now a new factor reflecting the adhesion force between cells. The critical value n_0 is assumed to satisfy $0 < n_0 < 2$. By Propositions 1 and 2 in [37], it is known that the solution satisfies $0 \leq n(x, t) \leq 2$ for all $t > 0$ and $x \in (-\infty, +\infty)$, if $0 \leq n(x, 0) \leq 2$ for all $x \in (-\infty, +\infty)$.

In the spatially homogeneous situation, the steady states of (2.6) are $N^* = 0$ and $N^* = n_0$. This property gives a suggestion to investigate the traveling wavefront solutions of (2.6) connecting $N^* = 0$ and $N^* = n_0$.

Chapter 3

Existence of wave patterns for small α

This chapter studies the existence of traveling wave patterns of (2.6) and investigates the critical wave speed by using the standard linear stability analysis.

3.1 Critical wave speed

Recall that a traveling wave solution with a wave speed c refers to a pair (N, c) , where $N(z) = N(x + ct)$ is a nontrivial and bounded solution. Here c is a positive constant. If $N(\pm\infty)$ exist and $N(-\infty) \neq N(+\infty)$, (N, c) is called a wavefront. To construct the traveling wave solutions of (2.6), we assume $n(x, t) = N(z)$, $z = x + ct$ and additionally set the following boundary conditions:

$$\begin{cases} N(-\infty) = 0, \\ N(+\infty) = n_0. \end{cases} \quad (3.1)$$

Substituting the proposed traveling wave-form solution $N(z) = N(x + ct)$ into (2.6), a second order ODE for $N(z)$ is obtained

$$DN''(z) - cN'(z) - \alpha \left[N(z) \int_{-1}^{+1} A(N(z + x_0)) \omega(x_0) dx_0 \right]' + \mu N(z) \left(1 - \frac{N(z)}{n_0} \right) = 0, \quad (3.2)$$

where

$$\begin{cases} A(N(z + x_0)) = \max\{N(z + x_0)[2 - N(z + x_0)], 0\}, \\ \omega(x_0) = \text{sign}(x_0). \end{cases} \quad (3.3)$$

We shall find the traveling wave solutions $N(z)$ of equation (3.2) with boundary conditions (3.1).

A standard linear stability analysis of the uniform steady state $N^* = 0$ can give the critical wave speed c . Indeed, letting $N' = X$, we obtain the following ODE system of N and X :

$$\begin{cases} N' = X, \\ X' = \frac{c}{D}X + \frac{\alpha}{D} \left[N(z) \int_{-1}^{+1} A(N(z + x_0)) \omega(x_0) dx_0 \right]' - \frac{\mu}{D}N(z) \left(1 - \frac{N(z)}{n_0} \right), \end{cases} \quad (3.4)$$

Hence the steady states of (3.4) are $(N, X) = (0, 0)$ and $(N, X) = (n_0, 0)$. After a linearization of system (3.4) at $(0, 0)$, we obtain the following linear ODE system of (N, X) :

$$\begin{pmatrix} N' \\ X' \end{pmatrix} = \begin{pmatrix} 0 & 1 \\ -\frac{\mu}{D} & \frac{c}{D} \end{pmatrix} \begin{pmatrix} N \\ X \end{pmatrix}. \quad (3.5)$$

To study the stability of $(0, 0)$, we need to determine the eigenvalues of the coefficient matrix in (3.5). The characteristic equation of this matrix is

$$\Delta(\lambda) = \lambda^2 - \frac{c}{D}\lambda + \frac{\mu}{D} = 0, \quad (3.6)$$

where λ is the eigenvalue.

To continue, we first introduce some terminologies of dynamical systems. In a two-dimensional phase portrait of dynamical systems, the stability of a steady state is determined by the eigenvalues of the Jacobian matrix. A steady state is a stable node, if the trajectories flow into the point in all directions; whereas it is an unstable node, if the trajectories flow to infinity in all directions. A steady state is a stable (an unstable) spiral, if trajectories spiral around the point as they approach (or recede). A steady state is a saddle point, if almost all trajectories initially flow into the point asymptotically to the stable eigenline with respect to the negative eigenvalue, then turn and flow out to infinity asymptotically to the unstable eigenline with respect to the positive eigenvalue.

For the existence of traveling wave solutions $N(z)$, we are interested only in the positive solutions going out from the origin (saddle point) and connecting to the other equilibrium n_0 (stable node). The critical wave speed c^* is the minimum wave speed for a traveling wavefront. We exclude the existence of unstable spiral manifolds of the origin and require

$$c \geq c^* = 2\sqrt{D\mu}. \quad (3.7)$$

3.2 Traveling wave solutions for $\alpha = 0$

Assuming $\alpha = 0$ in (2.6), we obtain the limiting model without the adhesion term. The result (3.7) for wavespeed is also true for this limiting case. By setting $\alpha = 0$, we have the following reaction-diffusion model:

$$\frac{\partial n(x, t)}{\partial t} = D \frac{\partial^2 n(x, t)}{\partial x^2} + \mu n \left(1 - \frac{n}{n_0} \right), \quad (3.8)$$

which is the well-known Fisher's equation with the logistic kinetics. Now let $n(x, t) = N_0(z) = N_0(x + ct)$ be the traveling wave solutions of (3.8), where $c \geq 0$ is the wave speed. Substituting the wavefront form $N_0(x + ct)$ into (3.8) yields a second order ODE with respect to N_0 :

$$DN_0'' - cN_0' + \mu N_0 \left(1 - \frac{N_0}{n_0}\right) = 0. \quad (3.9)$$

By the standard phase plane technique, Murray [31] has established the existence of traveling wave solutions for the Fisher equation (3.8): for any wave speed $c \geq 2\sqrt{D\mu}$, there exists a positive traveling wave solution $N_0(z)$ connecting the two fixed points 0 and n_0 , which satisfies the boundary conditions $N_0(-\infty) = 0$ and $N_0(+\infty) = n_0$. Furthermore, the traveling wavefront is strictly increasing, and $c_{min} = 2\sqrt{D\mu}$ is the minimal wave speed in this case.

3.3 Traveling wave solutions for α sufficiently small

Our purpose is to establish the existence of traveling wave solutions for (2.6) on the unbounded space domain $x \in (-\infty, +\infty)$ when the cell-adhesion coefficient α is not equal to zero. The approach used in this section is based on a combination of perturbation methods, the Fredholm theory, and the Banach fixed point theorem to handle the case when $\alpha (> 0)$ is small; see [32] and [33] for details.

3.3.1 Notations of spaces and norms

To start, we first introduce some notations of spaces and norms for later use. Let $C = C(\mathbf{R}, \mathbf{R})$ be the Banach space of continuous and bounded functions from \mathbf{R} to \mathbf{R} with the standard norm $\|\phi\|_C = \sup\{|\phi(t)|, t \in \mathbf{R}\}$. Furthermore, we denote

$C^1 = C^1(\mathbf{R}, \mathbf{R}) = \{\phi \in C : \phi' \in C\}$, $C^2 = \{\phi \in C : \phi'' \in C\}$, $C_0 = \{\phi \in C : \lim_{t \rightarrow \pm\infty} \phi = 0\}$, $C_0^1 = \{\phi \in C_0 : \phi' \in C_0\}$ with the corresponding norms defined, respectively, by

$$\|\phi\|_{C_0} = \|\phi\|_C, \quad \|\phi\|_{C^1} = \|\phi\|_{C_0^1} = \|\phi\|_C + \|\phi'\|_C,$$

and

$$\|\phi\|_{C^2} = \|\phi\|_C + \|\phi'\|_C + \|\phi''\|_C.$$

3.3.2 Approximation of wavefronts by using perturbation methods

For the case when α (> 0) is relatively small, we will prove the existence of traveling wave solutions $N(z)$ for (3.2) and show that such wavefronts can be approximated by the corresponding traveling wave N_0 of (3.9). Now assume

$$N = N_0 + V, \tag{3.10}$$

where $V(z)$ is a real function satisfying the boundary condition $V(\pm\infty) = 0$. Substituting (3.10) into (3.2), a differential equation for V is obtained

$$DV'' - cV' - V + E(V, N_0) = 0, \tag{3.11}$$

where

$$E(V, N_0) = \left(1 + \mu - \frac{2\mu N_0}{n_0}\right)V + R - G',$$

$$R = -\frac{\mu}{n_0}V^2, \quad (3.12)$$

$$G = (N_0 + V)S(N_0 + V) = \alpha(N_0 + V) \int_{-1}^{+1} A(N_0 + V)\omega(x_0)dx_0.$$

$A(N_0 + V)$ and $\omega(x_0)$ are defined in (3.3).

It is necessary to transform the differential equation (3.11) into an integral equation.

Since the equation

$$DV'' - cV' - V = 0$$

has two real characteristic roots:

$$\lambda_1 = \frac{c - \sqrt{c^2 + 4D}}{2D} < 0, \quad \lambda_2 = \frac{c + \sqrt{c^2 + 4D}}{2D} > 0, \quad (3.13)$$

the integral equation for $V(z)$ from (3.11) is then expressed by

$$\begin{aligned} V(z) &= \frac{1}{D(\lambda_2 - \lambda_1)} \int_{-\infty}^z e^{\lambda_1(z-s)} \left[\left(1 + \mu - \frac{2\mu N_0}{n_0}\right)V(s) + R - G' \right] ds \\ &\quad + \frac{1}{D(\lambda_2 - \lambda_1)} \int_z^{+\infty} e^{\lambda_2(z-s)} \left[\left(1 + \mu - \frac{2\mu N_0}{n_0}\right)V(s) + R - G' \right] ds \\ &= \frac{1}{D(\lambda_2 - \lambda_1)} \int_{-\infty}^z e^{\lambda_1(z-s)} \left[\left(1 + \mu - \frac{2\mu N_0}{n_0}\right)V(s) + R \right] ds \\ &\quad + \frac{1}{D(\lambda_2 - \lambda_1)} \int_z^{+\infty} e^{\lambda_2(z-s)} \left[\left(1 + \mu - \frac{2\mu N_0}{n_0}\right)V(s) + R \right] ds \\ &\quad + Q(z, V), \end{aligned} \quad (3.14)$$

where

$$Q(z, V) = \frac{-1}{D(\lambda_2 - \lambda_1)} \left[\int_{-\infty}^z e^{\lambda_1(z-s)} G' ds + \int_z^{+\infty} e^{\lambda_2(z-s)} G' ds \right]. \quad (3.15)$$

By integrating by parts, from (3.15), it yields that

$$Q(z, V) = \frac{-1}{D(\lambda_2 - \lambda_1)} \left[\lambda_1 \int_{-\infty}^z e^{\lambda_1(z-s)} G ds + \lambda_2 \int_z^{+\infty} e^{\lambda_2(z-s)} G ds \right]. \quad (3.16)$$

3.3.3 Demonstration of the existence of traveling waves for small α

In order to prove the existence of traveling wave solutions $N(x + ct)$ of (2.6) with relatively small α , it is necessary to establish the existence of a solution $V(z) \in C_0$ of (3.14). We define a linear operator $L : C_0 \rightarrow C_0$ given by

$$\begin{aligned} L(V(z)) = & V - \frac{1}{D(\lambda_2 - \lambda_1)} \int_{-\infty}^z e^{\lambda_1(z-s)} \left(1 + \mu - \frac{2\mu N_0}{n_0} \right) V(s) ds \\ & - \frac{1}{D(\lambda_2 - \lambda_1)} \int_z^{+\infty} e^{\lambda_2(z-s)} \left(1 + \mu - \frac{2\mu N_0}{n_0} \right) V(s) ds. \end{aligned} \quad (3.17)$$

Then we have the following lemma for L .

Lemma 3.1. $L(V(z)) \in C_0$ for any $V(z) \in C_0$.

Proof. $L(V(z))$ is well defined for any $z \in (-\infty, +\infty)$, where $\lambda_1 < 0$ and $\lambda_2 > 0$ are defined in (3.13). Applying L'Hopital's rule to (3.17), the limit of $L(V(z))$ as

$z \rightarrow +\infty$ is

$$\begin{aligned}
\lim_{z \rightarrow +\infty} L(V(z)) &= \lim_{z \rightarrow +\infty} V - \lim_{z \rightarrow +\infty} \frac{1}{D(\lambda_2 - \lambda_1)} \left(\frac{\int_{-\infty}^z e^{-\lambda_1 s} \left(1 + \mu - \frac{2\mu N_0}{n_0}\right) V(s) ds}{e^{-\lambda_1 z}} \right. \\
&\quad \left. + \frac{\int_z^{+\infty} e^{-\lambda_2 s} \left(1 + \mu - \frac{2\mu N_0}{n_0}\right) V(s) ds}{e^{-\lambda_2 z}} \right) \\
&= \lim_{z \rightarrow +\infty} V - \frac{1}{D(\lambda_2 - \lambda_1)} \lim_{z \rightarrow +\infty} \left(1 + \mu - \frac{2\mu N_0(z)}{n_0} \right) \\
&\quad \times \left(\frac{V(z)}{-\lambda_1} - \frac{V(z)}{-\lambda_2} \right) \\
&= 0 - \frac{1}{D(\lambda_2 - \lambda_1)} \left(1 + \mu - \frac{2\mu N_0(+\infty)}{n_0} \right) \left(\frac{0}{-\lambda_1} - \frac{0}{-\lambda_2} \right) \\
&= 0. \tag{3.18}
\end{aligned}$$

This result also holds when z tends to $-\infty$. The proof is complete.

By using the linear operator L defined above, equation (3.14) can be written as

$$L(V(z)) = \frac{1}{D(\lambda_2 - \lambda_1)} \left[\int_{-\infty}^z e^{\lambda_1(z-s)} R ds + \int_z^{+\infty} e^{\lambda_2(z-s)} R ds \right] + Q(z, V). \tag{3.19}$$

This means we need to verify the existence of a solution $V(z) \in C_0$ to the integral equation (3.19) in order to prove the existence of $N(z)$ to (2.6). We will apply the Banach fixed point theorem to show the existence of $V(z) \in C_0$. For this purpose, we first present some lemmas to estimate the terms in the right-hand side of (3.19).

3.3.3.1 Approximation of $R(V)$ and $Q(z, V)$

The following lemma is proved to approximate $R(V)$ defined in (3.12).

Lemma 3.2. *For each $\rho > 0$, there is a constant $\sigma > 0$ such that*

$$\|R(\phi) - R(\varphi)\|_{C_0} \leq \rho \|\phi - \varphi\|_{C_0} \quad (3.20)$$

and

$$\begin{aligned} & \int_{-\infty}^z e^{\lambda_1(z-s)} |R(\phi) - R(\varphi)| ds + \int_z^{+\infty} e^{\lambda_2(z-s)} |R(\phi) - R(\varphi)| ds \\ & \leq \rho \|\phi - \varphi\|_{C_0} \end{aligned} \quad (3.21)$$

for all $\phi, \varphi \in B(\sigma)$, where $B(\sigma)$ is the ball in C_0 with radius σ and center at the origin.

Proof. As we know,

$$\|R(\phi)\| = O(\|\phi\|_{C_0}^2), \text{ as } \|\phi\|_{C_0} \rightarrow 0. \quad (3.22)$$

Hence (3.20) and (3.21) follow from (3.22). The proof is complete.

The following lemma is proved to approximate $Q(z, V)$ defined in (3.16).

Lemma 3.3. *For any $\rho > 0$, there are constants $\delta, \sigma > 0$ such that*

$$|Q(z, V)| \leq O(\alpha) + O(\alpha \|V\|) + O(\alpha \|V\|^2) + O(\alpha \|V\|^3) \quad (3.23)$$

for any $V \in B(\sigma)$ and $\alpha \in (0, \delta)$, and

$$|Q(z, \phi) - Q(z, \varphi)| \leq \rho \|\phi - \varphi\|_{C_0} \quad (3.24)$$

for all $\phi, \varphi \in B(\sigma)$, where $B(\sigma)$ is the ball in C_0 with radius σ and center at the origin.

Proof. In (3.16), we have

$$\begin{aligned} G &= \alpha(N_0 + V) \int_{-1}^{+1} A(N_0 + V) \omega(x_0) dx_0 \\ &= \alpha(N_0 + V) \int_{-1}^{+1} \max\{(N_0 + V)[2 - (N_0 + V)], 0\} \text{sign}(x_0) dx_0. \end{aligned}$$

Then an estimate of G is obtained

$$|G(V)| \leq O(\alpha) + O(\alpha \|V\|) + O(\alpha \|V\|^2) + O(\alpha \|V\|^3). \quad (3.25)$$

Thus (3.23) and (3.24) follow from (3.25). The proof is complete.

3.3.3.2 Surjective mapping L

Recall that equation (3.19) is the integral equation transformed from (3.11). We now focus on the original differential equation (3.11) and define an operator $T : \Psi \in C^2 \rightarrow C$ from the linear part of (3.11) as follows:

$$T\Psi(z) = -c\Psi'(z) + D\Psi''(z) + \left(\mu - \frac{2\mu N_0}{n_0}\right)\Psi(z). \quad (3.26)$$

The formal adjoint equation of $T\Psi = 0$ for any $z \in (-\infty, +\infty)$, is given by

$$T^*\Phi(z) = c\Phi'(z) + D\Phi''(z) + \left(\mu - \frac{2\mu N_0}{n_0}\right)\Phi(z) = 0, \quad (3.27)$$

subject to the boundary condition $\Phi(\pm\infty) = 0$.

Lemma 3.4. *If $\Phi \in C$ is a solution of (3.27) and Φ is C^2 -smooth, then $\Phi(z) = 0$. Moreover, $R_s(T) = C$, where $R_s(T)$ is the range space of T .*

Proof. Note that $N_0(z) \rightarrow 0$ when $z \rightarrow -\infty$. Then we obtain an equation from

(3.27) given by

$$c\Phi'(z) + D\Phi''(z) + \mu\Phi(z) = 0, \quad (3.28)$$

as $z \rightarrow -\infty$. The corresponding characteristic equation of (3.28) is

$$D\lambda^2 + c\lambda + \mu = 0, \quad (3.29)$$

whose roots have negative real parts when $c \geq 2\sqrt{D\mu}$. Thus any bounded solution of (3.28) must be the zero solution when $z \rightarrow -\infty$. Any non-zero solution of (3.27) must therefore grow exponentially for large $|z|$ as $z \rightarrow -\infty$, which means that the only bounded solution of (3.27) is the zero solution. We have $\Phi = 0$ in order to satisfy the boundary condition $\Phi(\pm\infty) = 0$. Furthermore, by using the Fredholm theory (see Lemma 4.2 in [35]), we have that $R_s(T) = C$. The proof is complete.

Lemma 3.5. *For any given $\Theta \in C_0$, if Ψ is a bounded solution of $T\Psi = \Theta$, then $\Psi(z) \in C_0$.*

Proof. As $z \rightarrow +\infty$, the equation

$$-c\Psi'(z) + D\Psi''(z) + \left(\mu - \frac{2\mu N_0}{n_0}\right)\Psi(z) = \Theta \quad (3.30)$$

tends asymptotically to

$$-c\Psi'(z) + D\Psi''(z) - \mu\Psi(z) = 0. \quad (3.31)$$

The ω -limit set for (3.31) of every bounded solution is $\Psi = 0$, which implies, by Theorem 1.8 in [30], that every bounded solution of (3.30) satisfies

$$\lim_{z \rightarrow +\infty} \Psi(z) = 0.$$

Similarly, any bounded solution of (3.30) also satisfies

$$\lim_{z \rightarrow -\infty} \Psi(z) = 0.$$

The proof is complete.

Lemma 3.6. $R_s(L) = C_0$, where $R_s(L)$ is the range space of L , and L is the operator defined in (3.17). That is, for any $Z \in C_0$, there exists a $V \in C_0$ such that

$$\begin{aligned} V(z) - \frac{1}{D(\lambda_2 - \lambda_1)} \int_{-\infty}^z e^{\lambda_1(z-s)} \left(1 + \mu - \frac{2\mu N_0}{n_0}\right) V(s) ds \\ - \frac{1}{D(\lambda_2 - \lambda_1)} \int_z^{+\infty} e^{\lambda_2(z-s)} \left(1 + \mu - \frac{2\mu N_0}{n_0}\right) V(s) ds = Z(z). \end{aligned} \quad (3.32)$$

Proof. Let $\eta(z) = V(z) - Z(z)$ and substitute this into (3.32), the following equation for η is then obtained:

$$\begin{aligned} \eta(z) = & \frac{1}{D(\lambda_2 - \lambda_1)} \int_{-\infty}^z e^{\lambda_1(z-s)} \left(1 + \mu - \frac{2\mu N_0}{n_0}\right) (\eta + Z) ds \\ & + \frac{1}{D(\lambda_2 - \lambda_1)} \int_z^{+\infty} e^{\lambda_2(z-s)} \left(1 + \mu - \frac{2\mu N_0}{n_0}\right) (\eta + Z) ds. \end{aligned} \quad (3.33)$$

Transforming (3.33) to the corresponding differential equation yields

$$-c\eta'(z) + D\eta''(z) + \left(\mu - \frac{2\mu N_0}{n_0}\right)\eta(z) = -\left(1 + \mu - \frac{2\mu N_0}{n_0}\right)Z(z), \quad (3.34)$$

which is exactly the form $T\eta(z) = -\left(1 + \mu - \frac{2\mu N_0}{n_0}\right)Z(z)$. Since the righthand side of (3.34) satisfies

$$-\left(1 + \mu - \frac{2\mu N_0}{n_0}\right)Z(z) \in C_0$$

and $R_s(T) = C$ is given by Lemma 3.4, we conclude by Lemma 3.5 that there exists a solution $\eta(z)$ satisfying (3.34) and $\eta(\pm\infty) = 0$. Therefore, we have $V = \eta + Z \in C_0$.

The proof is complete.

By Lemmas 3.4, 3.5 and 3.6, we know that $L : C_0 \rightarrow C_0$ is a surjective (onto) mapping.

3.3.3.3 The main theorem

Now we will establish the existence of a solution $V \in C_0$ to the integral equation (3.19) and prove the main theorem.

Theorem 3.1. *For any $c \geq 2\sqrt{D\mu}$, there exists a constant $\delta = \delta(c) > 0$ so that for any $\alpha \in [0, \delta]$, equation (2.6) has a traveling wave solution $n(t, x) = N(x + ct)$ satisfying the boundary condition (3.1), where c is the wave speed.*

Proof. To show the existence of a solution $V \in C_0$ to (3.19), we restrict the operator L to a quotient space. Let $N(L)$ be the null space of operator L . Using Lemma 5.1 in [12], there exists a subspace $N^\perp(L)$ in C_0 so that

$$C_0 = N^\perp(L) \oplus N(L),$$

where $N^\perp(L)$ is obviously a Banach space. We then restrict the operator L to $N^\perp(L)$ by defining $P = L|_{N^\perp(L)}$. Hence the mapping $P : N^\perp(L) \rightarrow C_0$ is a bijective bounded linear operator. By the Banach inverse operator theorem, there exists a linear bounded inverse operator $P^{-1} : C_0 \rightarrow N^\perp(L)$. Then the equation (3.19) is written in the form of P

$$P(V(z)) = \frac{1}{D(\lambda_2 - \lambda_1)} \left[\int_{-\infty}^z e^{\lambda_1(z-s)} R ds + \int_z^{+\infty} e^{\lambda_2(z-s)} R ds \right] + Q(z, V). \quad (3.35)$$

Since P is invertible, equation (3.35) becomes

$$V(z) = F(V(z)),$$

where

$$\begin{aligned} F(V(z)) := & P^{-1} \left(\frac{1}{D(\lambda_2 - \lambda_1)} \left[\int_{-\infty}^z e^{\lambda_1(z-s)} R ds + \int_z^{+\infty} e^{\lambda_2(z-s)} R ds \right] \right. \\ & \left. + Q(z, V) \right). \end{aligned} \quad (3.36)$$

From Lemmas 3.2 and 3.3, we know that

$$\|F(V(z))\| \leq \|P^{-1}\| \left[O(\|V\|^2) + O(\alpha) + O(\alpha \|V\|) + O(\alpha \|V\|^2) + O(\alpha \|V\|^3) \right].$$

Evidently, $\|P^{-1}\|$ is independent of α . Thus there exist small constants $\delta, \sigma > 0$ and $0 < \rho < 1$ such that for $V, \varphi, \phi \in B(\sigma) \cap N^\perp(L)$ and $\alpha \in (0, \delta)$, we have the following estimate:

$$\begin{aligned} \|F(V(z))\| & \leq \|P^{-1}\| \left[O(\|V\|^2) + O(\alpha) + O(\alpha \|V\|) + O(\alpha \|V\|^2) + O(\alpha \|V\|^3) \right] \\ & = \|P^{-1}\| \left[O(\alpha) + \|V\| (O(\alpha) + O(\|V\|) + O(\alpha \|V\|) + O(\alpha \|V\|^2)) \right] \\ & \leq \frac{1}{3}(\sigma + \|V\|) \leq \sigma, \end{aligned} \quad (3.37)$$

and

$$\|F(z, \phi) - F(z, \varphi)\| \leq \rho \|\phi - \varphi\|.$$

Therefore, $F(z, V)$ is a uniform contractive mapping for $V \in B(\sigma) \cap N^\perp(L)$. Applying the Banach contraction principle, we conclude that for $\alpha \in (0, \delta)$, there exists a unique

solution $V \in B(\sigma) \cap N^\perp(L)$ of equation (3.19). Returning to the original variable, we then determine that $N = N_0 + V$ is a traveling wave solution of (2.6) with the wave speed $c \geq 2\sqrt{D\mu}$ connecting 0 to n_0 . The proof is complete.

Chapter 4

Application to cancer invasion

Having confirmed that traveling wave solutions are possible in the non-local reaction-diffusion model for cell adhesion, this chapter investigates the application modeling cancer invasion within a matrix environment. This cancer invasion model incorporates the important biological effects of cell proliferation and proteolysis by the surrounding extracellular matrix, along with both cell-cell and cell-matrix adhesion. We consider the non-local model system for cancer invasion in one space dimension in Sherratt *et al.* [37], which was based on the model proposed by Armstrong *et al.* [4].

4.1 Introduction of the cancer invasion model

To begin with, we assume that tumor cells adhere both to each other (cell-cell adhesion) and to the surrounding extracellular matrix (cell-matrix adhesion), and that the cell movement is driven entirely by the adhesive binding force.

As in Sherratt *et al.* [37], the model discussed here has time- and space-dependent variables, where $n(x, t)$ is the tumor cell (cancer cell) density and $m(x, t)$ is the density of the extracellular matrix. For more detail about the model establishment, see [34]

and [37]. The continuum non-local model for cancer invasion is given by

$$\begin{cases} \frac{\partial n(x,t)}{\partial t} = D \frac{\partial^2 n}{\partial x^2} - \frac{\partial}{\partial x} [n(x,t)K(n(x,t), m(x,t))] + f(n), \\ \frac{\partial m(x,t)}{\partial t} = -\gamma n m^2, \end{cases} \quad (4.1)$$

with positive constants $\alpha, \beta, \gamma, \chi$, and D , where

$$\begin{aligned} K(n(x,t), m(x,t)) &= \chi \int_{-1}^{+1} \bar{A}(n(x+x_0, t), m(x+x_0, t)) \omega(x_0) dx_0 \\ &= \chi \int_{-1}^{+1} [\alpha n(x+x_0, t) + \beta m(x+x_0, t)] \\ &\quad \cdot g(n(x+x_0, t) + m(x+x_0, t)) \omega(x_0) dx_0. \end{aligned} \quad (4.2)$$

Biologically, the second equation in (4.1) describes the degradation of extracellular matrix caused by proteolytic enzymes, such as the urokinase-type plasminogen activator (uPA) and matrix metalloproteinases (MMPs). See Zigrino *et al.* [39] for a more detailed biological interpretation of the cancer invasion process.

The parameter D is the diffusion coefficient implying the influence of the tumor cell's diffusive process. The dimensionless parameters α and β are positive constants reflecting the strength of the cell-cell adhesion and the cell-matrix adhesion, respectively. γ is the matrix degradation rate.

Numerical simulations in [34] and [37] showed that in a bounded domain, the non-invasive tumor cell growth occurs with sufficiently strong cell-cell adhesion and/or sufficiently weak cell-matrix adhesion ($\alpha > \beta$). The population of tumor cells increases towards its carrying capacity without expansion outside the initial space range. However, when the cell-matrix adhesion is relatively stronger than the cell-cell adhesion ($\alpha < \beta$), the cell population grows and expands by the force of cell-matrix adhesion to the matrix, which is the invasive cell growth. The surrounding extracellular matrix

is degraded by proteolytic enzymes produced by the tumor cells. Figure 2 in [34] and Figure 5 in [37] presented the invasion speed as a function of cell-cell adhesion coefficient α and cell-matrix adhesion coefficient β .

4.2 Description of notation

The integral $K(n(x, t), m(x, t))$ expressed in (4.2) is the non-local adhesion term, encompassing both cell-cell adhesion and cell-matrix adhesion. Here we add the coefficient χ within the expression of $K(n(x, t), m(x, t))$ to describe the total effect of adhesion strengths of both cell-cell and cell-matrix. Chapter 5 studies the significant impact of χ on the existence of traveling waves to system (4.1). Here $\bar{A}(n(x + x_0, t), m(x + x_0, t))$ within the integral represents the local adhesive force as in chapter 2 created by both cell-cell and cell-matrix at position x with a distance x_0 away.

The function $g(\xi)$ in (4.2) implies the decreasing effect in local adhesive force with cell and matrix densities. Sherratt *et al.* [37] assumed a linear decreasing function for the force and provided a condition for $g(\xi)$ to satisfy the required boundedness:

$$g(\xi) > 0 \quad \text{and bounded on} \quad 0 < \xi < 2, \quad g(\xi) = 0 \quad \text{on} \quad \xi \geq 2.$$

Hence the rescaled form of $g(n(x + x_0, t), m(x + x_0, t))$ in (4.2) is given as follows:

$$g(n(x + x_0, t), m(x + x_0, t)) = \max\{2 - n(x + x_0, t) - m(x + x_0, t), 0\}, \quad (4.3)$$

where the dimensionless cell density 2 corresponds to the crowding capacity of tumor cells.

The function $\omega(x_0)$ in (4.2) describes how the direction and magnitude of the adhesive

force (both cell-cell and cell-matrix adhesion force) generated by the cells vary over the cell sensing region. As mentioned in chapter 2, $\omega(x_0)$ is an odd function, since the adhesive forces are always directed towards the cell centers; see [4]. Sherrate *et al.* [37] set a condition on $\omega(x_0)$ in their model derivation, which is

$$\int_0^1 \omega(x_0) dx_0 = 1 \quad \text{and} \quad \omega(x_0) \geq 0 \quad \text{on} \quad x_0 \geq 0.$$

After rescaling, the function $\omega(x_0)$ with uniform adhesive property becomes $\omega(x_0) = \text{sign}(x_0)$.

For the tumor cell kinetics, Sherrate *et al.* [37] chose the same expression as in chapter 2 using the logistic function: $f(n) = \mu n(1 - \frac{n}{n_0})$, which satisfies the condition:

$$f(0) = f(n_0) = 0 \quad \text{for some} \quad n_0 \in (0, 2),$$

$$f(n) > 0 \quad \text{on} \quad 0 < n < n_0,$$

$$f(n) < 0 \quad \text{on} \quad n > n_0.$$

The parameters μ and n_0 have the same meaning as in chapter 2.

4.3 Dimensionless model for cancer invasion

From all above, the non-local system (4.1) of cancer invasion therefore becomes

$$\begin{cases} \frac{\partial n(x,t)}{\partial t} = D \frac{\partial^2 n}{\partial x^2} - \chi \frac{\partial}{\partial x} [n \int_{-1}^{+1} (\alpha n + \beta m) g(n+m) \omega(x_0) dx_0] + \mu n(1 - \frac{n}{n_0}), \\ \frac{\partial m(x,t)}{\partial t} = -\gamma n m^2, \end{cases} \quad (4.4)$$

where functions $g(n + m)$ and $\omega(x_0)$ are defined as before. Specifically, the coefficient χ in (4.4) is a dimensionless adhesion parameter, incorporating both cell-cell and cell-matrix adhesion. The carrying capacity of tumor cells in this model is the constant 2 as in chapter 2, and n_0 also satisfies $0 < n_0 < 2$. The boundedness of the solutions is thus known from [37].

System (4.4) also has two spatially homogeneous solutions $(0, H)$ and $(n_0, 0)$, where H is any given positive constant. We will look for the traveling wavefront solutions of (4.4) with $0 \leq n(x, t) \leq 2$ and $0 \leq m(x, t) \leq H$; see [37].

Chapter 5

Wave solutions of the system (4.4) for small χ

Since Sherratt *et al.* [37] and Painter *et al.* [34] have obtained numerical figures and analyzed the evolution of traveling wavefronts on a bounded domain, this chapter furthers their study by rigorously proving the existence of wavefronts. Based on the approach used in chapter 3 for cell adhesion model, we apply the perturbation methods and the Banach contraction mapping principle to show the existence of traveling wavefronts on the unbounded domain, where cell-cell adhesion occurs in cancer invasion along with cell-matrix adhesion for small coefficient χ .

5.1 Traveling wave solutions for the limiting system when $\chi = 0$

To start, the limiting case when $\chi = 0$ is obtained by the following diffusion model:

$$\begin{cases} \frac{\partial n(x,t)}{\partial t} = D \frac{\partial^2 n}{\partial x^2} + \mu n \left(1 - \frac{n}{n_0}\right), \\ \frac{\partial m(x,t)}{\partial t} = -\gamma n m^2. \end{cases} \quad (5.1)$$

To see the traveling wave solutions for system (5.1), let $n(x, t) = N_0(z) = N_0(x + ct)$ and $m(x, t) = M_0(z) = M_0(x + ct)$, where $c > 0$ is the wave speed. Then we obtain the following second order ODE system for $N_0(z)$ and $M_0(z)$:

$$\begin{cases} DN_0'' - cN_0' + \mu N_0 \left(1 - \frac{N_0}{n_0}\right) = 0, \\ cM_0' = -\gamma N_0 M_0^2. \end{cases} \quad (5.2)$$

Furthermore, we impose the following boundary conditions:

$$\begin{cases} N_0(-\infty) = 0, \\ M_0(-\infty) = H, \end{cases} \quad \text{and} \quad \begin{cases} N_0(+\infty) = n_0, \\ M_0(+\infty) = 0. \end{cases} \quad (5.3)$$

Note that the first equation of (5.1) is decoupled from the second one. This first equation is the well-know Fisher's equation with the logistic kinetic. As mentioned before, Murray has established the existence of traveling wave solutions N_0 for the Fisher equation with the wave speed $c \geq 2\sqrt{D\mu}$.

We can obtain M_0 from the second equation of (5.2) by using N_0 . The second equation

of (5.2) is a first order ODE for M_0 . Solving this equation yields

$$M_0(z) = \frac{1}{\frac{1}{H} + \frac{\gamma}{c} \int_{-\infty}^z N_0(s) ds}.$$

Using the fact that $N_0(-\infty) = 0$ and $N_0(+\infty) = n_0$, it is evident that

$$\lim_{z \rightarrow -\infty} M_0 = H \quad \text{and} \quad \lim_{z \rightarrow +\infty} M_0 = 0.$$

Therefore, both $N_0(z)$ and $M_0(z)$ satisfy the boundary conditions (5.3), and the wave speed satisfies $c \geq 2\sqrt{D\mu}$.

The following theorem is expressed for the existence of traveling wave solutions to system (5.2).

Theorem 5.1. *For any wave speed $c \geq 2\sqrt{D\mu}$, there exists a heteroclinic solution of system (5.2) connecting the fixed points $(0, H)$ with $(n_0, 0)$.*

Note that $M'_0 < 0$ in the second equation of (5.2). Thus M_0 is strictly decreasing and bounded.

5.2 Traveling wave solutions for χ sufficiently small

For relatively small $\chi > 0$, we will prove the existence of wave solutions $n(x, t) = N(z) = N(x+ct)$ and $m(x, t) = M(z) = M(x+ct)$ for system (4.4), when $c \geq 2\sqrt{D\mu}$. Substituting the proposed solutions into (4.4), we obtain a second order ODE system for $N(z)$ and $M(z)$ as follows:

$$\begin{cases} DN'' - cN' - [N \cdot K(N, M)]' + \mu N \left(1 - \frac{N}{n_0}\right) = 0, \\ cM' = -\gamma NM^2, \end{cases} \quad (5.4)$$

with the following boundary conditions:

$$\begin{cases} N(-\infty) = 0, \\ M(-\infty) = H, \end{cases} \quad \text{and} \quad \begin{cases} N(+\infty) = n_0, \\ M(+\infty) = 0, \end{cases} \quad (5.5)$$

where

$$K(N, M) = \chi \int_{-1}^{+1} [\alpha N(z + x_0) + \beta M(z + x_0)] \cdot g(N(z + x_0) + M(z + x_0)) \omega(x_0) dx_0.$$

5.2.1 Approximation of wavefronts by using perturbation methods

To approximate the traveling wave solutions $N(z)$ and $M(z)$ of system (4.4) by N_0 and M_0 , let

$$\begin{cases} N = N_0 + W_1, \\ M = M_0 + W_2, \end{cases} \quad (5.6)$$

where W_1 and W_2 are two unknown real functions that are subject to the boundary conditions:

$$W_i(\pm\infty) = 0, \quad i = 1, 2.$$

In order to construct the traveling wave solutions $N(z)$ and $M(z)$ for system (4.4), it is necessary to verify the existence of W_1 and W_2 . We first consider the first equation of system (5.4). Substituting (5.6) into the first equation of (5.4) yields a second order ODE for W_1 :

$$DW_1'' - cW_1' - W_1 + E_1(W_1, W_2, N_0, M_0) = 0, \quad (5.7)$$

where

$$E_1(W_1, W_2, N_0, M_0) = \left(1 + \mu - \frac{2\mu N_0}{n_0}\right) W_1 + R_1 - (\bar{G})',$$

$$R_1 = -\frac{\mu}{n_0} W_1^2,$$

and

$$\begin{aligned} \bar{G} &= (N_0 + W_1)K(N_0 + W_1, M_0 + W_2) \\ &= \chi(N_0 + W_1) \int_{-1}^{+1} \bar{A}(N_0 + W_1, M_0 + W_2) \omega(x_0) dx_0. \end{aligned}$$

Note that in the above equations, we have

$$\bar{A}(N_0 + W_1, M_0 + W_2) = [\alpha(N_0 + W_1) + \beta(M_0 + W_2)] \cdot g(N_0 + W_1 + M_0 + W_2),$$

where

$$g(N_0 + W_1 + M_0 + W_2) = \max\{2 - (N_0 + W_1) - (M_0 + W_2), 0\}.$$

The integral equation for W_1 from (5.7) is expressed by

$$\begin{aligned}
W_1(z) &= \frac{1}{D(\lambda_2 - \lambda_1)} \int_{-\infty}^z e^{\lambda_1(z-s)} \left[\left(1 + \mu - \frac{2\mu N_0}{n_0} \right) W_1(s) + R_1 - (\overline{G})' \right] ds \\
&\quad + \frac{1}{D(\lambda_2 - \lambda_1)} \int_z^{+\infty} e^{\lambda_2(z-s)} \left[\left(1 + \mu - \frac{2\mu N_0}{n_0} \right) W_1(s) + R_1 - (\overline{G})' \right] ds \\
&= \frac{1}{D(\lambda_2 - \lambda_1)} \int_{-\infty}^z e^{\lambda_1(z-s)} \left[\left(1 + \mu - \frac{2\mu N_0}{n_0} \right) W_1(s) + R_1 \right] ds \\
&\quad + \frac{1}{D(\lambda_2 - \lambda_1)} \int_z^{+\infty} e^{\lambda_2(z-s)} \left[\left(1 + \mu - \frac{2\mu N_0}{n_0} \right) W_1(s) + R_1 \right] ds \\
&\quad + Q_1(z, W_1, W_2), \tag{5.8}
\end{aligned}$$

where

$$Q_1(z, W_1, W_2) = \frac{-1}{D(\lambda_2 - \lambda_1)} \left[\int_{-\infty}^z e^{\lambda_1(z-s)} (\overline{G})' ds + \int_z^{+\infty} e^{\lambda_2(z-s)} (\overline{G})' ds \right], \tag{5.9}$$

and λ_1, λ_2 are defined in (3.13). Integrating by parts yields the following expression for $Q_1(z, W_1, W_2)$:

$$Q_1(z, W_1, W_2) = \frac{-1}{D(\lambda_2 - \lambda_1)} \left[\lambda_1 \int_{-\infty}^z e^{\lambda_1(z-s)} \overline{G} ds + \lambda_2 \int_z^{+\infty} e^{\lambda_2(z-s)} \overline{G} ds \right]. \tag{5.10}$$

Therefore, the integral equation (5.8) of W_1 is now expressed by using both variables W_1 and W_2 . This is different from the equation of V in (3.14) which is given only by V itself. As we know, the second equation in (5.4) is an ordinary differential equation for M , from which we obtain

$$M = M_0 + W_2 = \frac{1}{\frac{1}{H} + \frac{2}{c} \int_{-\infty}^z (N_0(s) + W_1(s)) ds}. \tag{5.11}$$

Then W_2 is written in terms of W_1 by the following equation:

$$W_2 = \frac{1}{\frac{1}{H} + \frac{\gamma}{c} \int_{-\infty}^z (N_0(s) + W_1(s)) ds} - M_0, \quad (5.12)$$

where M_0, N_0 are the given traveling wave solutions of the limiting system (5.1).

Hence after a substitution, we denote $Q_1(z, W_1, W_2) = Q_1(z, W_1)$ in (5.8).

5.2.2 Demonstration of the existence of traveling waves for small χ

In order to establish the existence of a solution $W_1 \in C_0$ for the integral equation (5.8), we now define a linear operator $L_1 : C_0 \rightarrow C_0$ as follows:

$$\begin{aligned} L_1(W_1(z)) &= W_1 - \frac{1}{D(\lambda_2 - \lambda_1)} \int_{-\infty}^z e^{\lambda_1(z-s)} \left(1 + \mu - \frac{2\mu N_0}{n_0}\right) W_1(s) ds \\ &\quad - \frac{1}{D(\lambda_2 - \lambda_1)} \int_z^{\infty} e^{\lambda_2(z-s)} \left(1 + \mu - \frac{2\mu N_0}{n_0}\right) W_1(s) ds. \end{aligned} \quad (5.13)$$

As in the proof of Lemma 3.1, $L_1(W_1(z))$ is well defined for any $z \in (-\infty, +\infty)$, and $L_1(W_1(z)) \in C_0$ when $W_1(z) \in C_0$.

By using the linear operator L_1 defined above, equation (5.8) can be rewritten as

$$L_1(W_1(z)) = \frac{1}{D(\lambda_2 - \lambda_1)} \left[\int_{-\infty}^z e^{\lambda_1(z-s)} R_1 ds + \int_z^{+\infty} e^{\lambda_2(z-s)} R_1 ds \right] + Q_1(z, W_1). \quad (5.14)$$

Therefore, it is necessary to verify the existence of $W_1 \in C_0$ for the integral equation (5.14). Before presenting the result, we need to estimate the nonlinear terms in the right-hand side of (5.14) by the following lemmas.

5.2.2.1 Approximation of $R_1(W_1)$ and $Q_1(z, W_1)$

The following lemma approximates $R_1(W_1)$ as defined above.

Lemma 5.1. *For each $\rho > 0$, there is a constant $\sigma > 0$ such that*

$$\|R_1(\phi) - R_1(\varphi)\|_{C_0} \leq \rho \|\phi - \varphi\|_{C_0} \quad (5.15)$$

and

$$\begin{aligned} & \int_{-\infty}^z e^{\lambda_1(z-s)} |R_1(\phi) - R_1(\varphi)| ds + \int_z^{+\infty} e^{\lambda_2(z-s)} |R_1(\phi) - R_1(\varphi)| ds \\ & \leq \rho \|\phi - \varphi\|_{C_0} \end{aligned} \quad (5.16)$$

for all $\phi, \varphi \in B(\sigma)$, where $B(\sigma)$ is the ball in C_0 with radius σ and center at the origin.

Proof. We have

$$\|R_1(\phi)\| = O(\|\phi\|_{C_0}^2), \text{ as } \|\phi\|_{C_0} \rightarrow 0, \quad (5.17)$$

Therefore, (5.15) and (5.16) follow from (5.17). The proof is complete.

For the estimation of $Q_1(z, W_1)$ in (5.14), we need an analysis of the second equation in (5.4).

Lemma 5.2. *For any $\rho > 0$, there are constants $\delta, \sigma > 0$ such that*

$$|Q_1(z, W_1)| \leq O(\chi) + O(\chi \|W_1\|) + O(\chi \|W_1\|^2) + O(\chi \|W_1\|^3) \quad (5.18)$$

for any $W_1 \in B(\sigma)$ and $\chi \in (0, \delta)$, and

$$|Q_1(z, \phi) - Q_1(z, \varphi)| \leq \rho \|\phi - \varphi\|_{C_0} \quad (5.19)$$

for all $\phi, \varphi \in B(\sigma)$, where $B(\sigma)$ is the ball in $C_0 \cap L^1(-\infty, +\infty)$ with radius σ and center at the origin.

Proof. From equation (5.11), M is obtained

$$M = \frac{1}{\frac{1}{H} + \frac{\gamma}{c} \int_{-\infty}^z (N_0(s) + W_1(s)) ds}, \quad (5.20)$$

from which we obtain

$$\frac{1}{\frac{1}{H} + \frac{\gamma}{c} \int_{-\infty}^{+\infty} N_0(s) ds + \frac{\gamma}{c} \int_{-\infty}^z W_1(s) ds} \leq M \leq \frac{1}{\frac{1}{H} + \frac{\gamma}{c} \int_{-\infty}^z W_1(s) ds}. \quad (5.21)$$

As we know, $W_1 \in B(\sigma) \in L^1(-\infty, +\infty)$. Choosing a ball $B(\sigma)$ in $L^1(-\infty, +\infty)$ with radius σ small such that

$$-\sigma \leq - \int_{-\infty}^z |W_1| ds \leq \int_{-\infty}^z W_1 ds \leq \sigma$$

and

$$\frac{1}{H} - \frac{\gamma}{c} \sigma > 0.$$

Then it is evident that

$$0 = \frac{1}{\frac{1}{H} + \frac{\gamma}{c} \int_{-\infty}^{+\infty} N_0(s) ds + \frac{\gamma}{c} \sigma} \leq M \leq \frac{1}{\frac{1}{H} + \frac{\gamma}{c} \int_{-\infty}^z W_1(s) ds} \leq \frac{1}{\frac{1}{H} - \frac{\gamma}{c} \sigma}.$$

Thus from (5.10), we have

$$\begin{aligned}\bar{G} &= \chi(N_0 + W_1) \int_{-1}^{+1} \bar{A}(N_0 + W_1, M_0 + W_2) \omega(x_0) dx_0 \\ &= \chi(N_0 + W_1) \int_{-1}^{+1} [\alpha(N_0 + W_1) + \beta M] \\ &\quad \cdot \max\{2 - (N_0 + W_1) - M, 0\} \omega(x_0) dx_0,\end{aligned}$$

which implies that

$$|Q_1(z, W_1)| \leq O(\chi) + O(\chi \|W_1\|) + O(\chi \|W_1\|^2) + O(\chi \|W_1\|^3), \quad (5.22)$$

for any $W_1 \in B(\sigma)$. (5.19) follows directly from (5.22). The proof is complete.

5.2.2.2 The main theorem

With all the lemmas above, we now give the existence of a solution $W_1 \in C_0 \cap L^1(-\infty, +\infty)$ for the integral equation (5.14) by applying the Banach fixed point theorem. The existence of a solution W_2 can be obtained from (5.12) by using W_1 . The following theorem presents the existence of traveling wave solutions for system (4.4) with relatively small χ .

Theorem 5.2. *For any $c \geq 2\sqrt{D\mu}$, there exists a constant $\delta = \delta(c) > 0$ so that for any $\chi \in [0, \delta]$, system (4.4) has traveling wave solutions $n(t, x) = N(x + ct)$ and $m(t, x) = M(x + ct)$ satisfying the boundary conditions (5.5).*

Proof. As we mentioned above, the existence of $N(z)$ and $M(z)$ directly follows from the existence of W_1 and W_2 . In this proof, we first establish the existence of W_1 in the integral equation (5.14).

Focusing on the original differential equation (5.7), we define an operation: $T_1 : \Psi \in$

$C^2 \rightarrow C$ from the linear part of (5.7) as

$$T_1\Psi(z) = -c\Psi'(z) + D\Psi''(z) + \left(\mu - \frac{2\mu N_0}{n_0}\right)\Psi(z). \quad (5.23)$$

The formal adjoint equation of $T_1\Psi = 0$ for any $z \in (-\infty, +\infty)$ is given by

$$T_1^*\Phi(z) = c\Phi'(z) + D\Phi''(z) + \left(\mu - \frac{2\mu N_0}{n_0}\right)\Phi(z) = 0, \quad (5.24)$$

subject to the boundary condition $\Phi(\pm\infty) = 0$.

Using the same methods and proofs as above in Lemmas 3.4, 3.5, 3.6, we have the following three claims.

Claim 1. If $\Phi \in C$ is a solution of (5.24) and Φ is C^2 -smooth, then $\Phi(z) = 0$. Moreover, $R_s(T_1) = C$, where $R_s(T_1)$ is the range space of T_1 .

Claim 2. If Ψ is a bounded solution of $T_1\Psi = \Theta$ for any given $\Theta \in C_0$, then $\Psi(z) \in C_0$.

Claim 3. $R_s(L_1) = C_0$, where $R_s(L_1)$ is the range space of L_1 , and L_1 is the operator defined in (5.13). That is, for any $Z \in C_0$, there exists a $W_1 \in C_0$ such that

$$\begin{aligned} W_1(z) - \frac{1}{D(\lambda_2 - \lambda_1)} \int_{-\infty}^z e^{\lambda_1(z-s)} \left(1 + \mu - \frac{2\mu N_0}{n_0}\right) W_1(s) ds \\ - \frac{1}{D(\lambda_2 - \lambda_1)} \int_z^{+\infty} e^{\lambda_2(z-s)} \left(1 + \mu - \frac{2\mu N_0}{n_0}\right) W_1(s) ds = Z(z). \end{aligned}$$

Hence the linear operator $L_1 : C_0 \rightarrow C_0$ is a surjective mapping. Now we restrict our operator L_1 to a quotient space. Let $N(L_1)$ be the null space of operator L_1 . Then there exists a subspace $N^\perp(L_1)$ in C_0 such that

$$C_0 = N^\perp(L_1) \oplus N(L_1),$$

where $N^\perp(L_1)$ is obviously a Banach space. We restrict the operator L_1 on $N^\perp(L_1)$ by defining $P_1 = L_1|_{N^\perp(L_1)}$. Since P_1 is also injective, the mapping $P_1 : N^\perp(L_1) \rightarrow C_0$ is a bijective bounded linear operator. Applying the Banach inverse operator theorem, there exists a linear bounded inverse operator $P_1^{-1} : C_0 \rightarrow N^\perp(L_1)$. Then (5.14) can be written in the form of P_1 as

$$P_1(W_1(z)) = \frac{1}{D(\lambda_2 - \lambda_1)} \left[\int_{-\infty}^z e^{\lambda_1(z-s)} R_1 ds + \int_z^{+\infty} e^{\lambda_2(z-s)} R_1 ds \right] + Q_1(z, W_1). \quad (5.25)$$

Since P_1 is invertible, equation (5.25) becomes

$$W_1(z) = F_1(W_1(z)), \quad (5.26)$$

where

$$F_1(W_1(z)) := P_1^{-1} \left(\frac{1}{D(\lambda_2 - \lambda_1)} \int_{-\infty}^z e^{\lambda_1(z-s)} R_1 ds + \frac{1}{D(\lambda_2 - \lambda_1)} \int_z^{+\infty} e^{\lambda_2(z-s)} R_1 ds + Q_1(z, W_1) \right). \quad (5.27)$$

By (5.9), Lemmas 5.1 and 5.2, there exist small constants $\delta, \sigma > 0$ and $0 < \rho < 1$ such that for $W_1, \varphi, \phi \in B(\sigma) \cap N^\perp(L_1)$ and $\chi \in (0, \delta)$, the following estimates holds:

$$\int_{-\infty}^{+\infty} |F_1(W_1(z))| dz < \sigma,$$

$$\begin{aligned}
\|F_1(W_1(z))\| &\leq \|P_1^{-1}\| \left[O(\|W_1\|^2) + O(\chi) + O(\chi \|W_1\|) + O(\chi \|W_1\|^2) \right. \\
&\quad \left. + O(\chi \|W_1\|^3) \right] \\
&= \|P_1^{-1}\| \left[O(\chi) + \|W_1\| (O(\chi) + O(\|W_1\|) + O(\chi \|W_1\|)) \right. \\
&\quad \left. + O(\chi \|W_1\|^2) \right] \\
&\leq \frac{1}{3}(\sigma + \|W_1\|) \leq \sigma, \tag{5.28}
\end{aligned}$$

and

$$\|F_1(z, \phi) - F_1(z, \varphi)\| \leq \rho \|\phi - \varphi\|, \tag{5.29}$$

where $\|P_1^{-1}\|$ is independent of χ . Therefore, $F_1(z, W_1)$ is a uniform contractive mapping for $W_1 \in B(\sigma) \cap N^\perp(L_1)$. Applying the Banach contraction mapping principle, we conclude that for $\chi \in (0, \delta)$, there exists a unique solution $W_1 \in B(\sigma) \cap N^\perp(L_1)$ for (5.14). Returning to the original variable, we then determine from (5.6) that $N = N_0 + W_1$ is a traveling wave solution of (4.4) connecting 0 to n_0 with the wave speed $c \geq 2\sqrt{D\mu}$ as discussed above. We then obtain M from (5.11). Therefore, for any $\chi \in [0, \delta]$, system (4.4) has traveling wave solutions $n(t, x) = N(x + ct) = N_0 + W_1$ and $m(t, x) = M(x + ct) = M_0 + W_2$ satisfying the boundary conditions (5.5), where the wave speed satisfies $c \geq 2\sqrt{D\mu}$. The proof is complete.

Chapter 6

Simulations

This chapter numerically simulates both the non-local cell adhesion model and its application to the cancer invasion model, by using the software MATLAB. We employ the central difference quotient approximation for all the partial derivatives in space. The choice of boundary conditions is dependent on the cell types and the problem requirement. For the sake of traveling wave solutions, all simulations in this chapter are performed with the Neumann boundary conditions on the symmetric spatial domain with respect to the origin. We pay particular attention to the terms near the boundaries by assuming that the cell densities are equal.

The key point in the simulations is the approximation of the non-local adhesion term. Armstrong *et al.* [4] and Gerisch [23] expanded the function within the integral as a Taylor series (see also [26]) so that the nonlocal term become localized. Here we focus on approximating the integral by using the Composite Trapezoidal rule and rewrite it as a sum. We apply the central difference scheme to the partial derivatives in space and the Forward Euler scheme in time.

6.1 Traveling waves of the cell adhesion model for small α

First we consider the integro-partial differential equation (2.6), which is the dimensionless model for the movement in cell aggregation. Having confirmed analytically that the traveling wave solutions exist for (2.6) with a sufficiently small cell adhesion coefficient α , we further investigate this through numerical simulation.

According to the results in [37], we may assume that $0 < n < 2$ with a proper choice of initial data, and thus it follows that

$$A(n(x + x_0, t)) = n(x + x_0, t)[2 - n(x + x_0, t)].$$

Hence the non-local reaction-diffusion model for cell adhesion (2.6) is written as

$$\begin{aligned} \frac{\partial n(x, t)}{\partial t} &= D \frac{\partial^2 n(x, t)}{\partial x^2} - \frac{\partial}{\partial x} [n(x, t)S(n(x, t))] + \mu n \left(1 - \frac{n}{n_0}\right) \\ &= D \frac{\partial^2 n(x, t)}{\partial x^2} - \alpha \frac{\partial}{\partial x} \left[n(x, t) \int_{-1}^1 A(n(x + x_0, t)) \omega(x_0) dx_0 \right] \\ &\quad + \mu n \left(1 - \frac{n}{n_0}\right) \\ &= D \frac{\partial^2 n(x, t)}{\partial x^2} - \alpha \frac{\partial}{\partial x} \left[n(x, t) \int_{-1}^1 n(x + x_0, t) [2 - n(x + x_0, t)] \right. \\ &\quad \left. \cdot \text{sign}(x_0) dx_0 \right] + \mu n \left(1 - \frac{n}{n_0}\right). \end{aligned} \tag{6.1}$$

6.1.1 The finite difference scheme of the cell adhesion model

We now start by discretizing the space interval $x \in [-l, l]$ (for some $l > 0$) and the time interval $t \in [0, t_{max}]$. Let $x_1 = -l, \dots, x_{N+1} = l$ be the $(N + 1)$ discretization

in space and $t_1 = 0, \dots, t_{M+1} = t_{max}$ be the $(M + 1)$ discretization in time, where $h = \frac{2l}{N}$ and $k = \frac{t_{max}}{M}$ are the step sizes for the space and time, respectively. Applying the central difference scheme in space and the Forward Euler scheme in time, the difference formula of (6.1) at location x_j and time t_i is given by

$$\begin{aligned}
\frac{n(x_j, t_{i+1}) - n(x_j, t_i)}{k} &= D \frac{\partial^2 n(x_j, t_i)}{\partial x_j^2} - \frac{\partial}{\partial x_j} [n(x_j, t_i) S(n(x_j, t_i))] \\
&\quad + \mu \left[n(x_j, t_i) \left(1 - \frac{n(x_j, t_i)}{n_0} \right) \right] \\
&= D \frac{n(x_{j+1}, t_i) - 2n(x_j, t_i) + n(x_{j-1}, t_i)}{h^2} \\
&\quad - \frac{n(x_{j+1}, t_i) S(n(x_{j+1}, t_i)) - n(x_{j-1}, t_i) S(n(x_{j-1}, t_i)))}{2h} \\
&\quad + \mu \left[n(x_j, t_i) \left(1 - \frac{n(x_j, t_i)}{n_0} \right) \right], \tag{6.2}
\end{aligned}$$

for $j = 1, 2, 3, \dots, N+1$, and $i = 1, 2, 3, \dots, M+1$, where $n_j = n(x_j, t_i)$ is the density of cells at location x_j and time t_i , and

$$S(n(x_j, t_i)) = \alpha \int_{-1}^1 A(n(x_j + x_0, t_i)) \text{sign}(x_0) dx_0. \tag{6.3}$$

To approximate $S(n(x_j, t_i))$, we choose the same discretization for x_0 with the step length h of x and apply the Composite Trapezoidal rule to obtain the sum of this

integral

$$\begin{aligned}
 S(n(x_j, t_i)) \approx & \frac{\alpha h}{2} \left[A(n(x_{j-\bar{N}}, t_i)) \text{sign}(-\bar{N}h) \right. \\
 & + 2 \sum_{s=-\bar{N}+1}^{\bar{N}-1} A(n(x_j + sh, t_i)) \text{sign}(sh) \\
 & \left. + A(n(x_{j+\bar{N}}, t_i)) \text{sign}(\bar{N}h) \right], \tag{6.4}
 \end{aligned}$$

where s denotes the discretization intervals. Here we choose h so that $\bar{N} = 1/h$ is a positive integer and there are $2\bar{N}$ intervals around x_j for the integration of the nonlocal term. Actually this interval number can be adjustable by changing the step size h .

Substituting (6.4) into (6.2), the finite difference approximation of (6.1) is thus given

by

$$\begin{aligned}
n(x_j, t_{i+1}) &= n(x_j, t_i) + Dk \frac{n(x_{j+1}, t_i) - 2n(x_j, t_i) + n(x_{j-1}, t_i)}{h^2} \\
&\quad - \frac{\alpha k}{4} \left[n(x_{j+1}, t_i) \left(A(n(x_{j+1-\bar{N}}, t_i)) \text{sign}(-\bar{N}h) \right. \right. \\
&\quad + 2 \sum_{s=-\bar{N}+1}^{\bar{N}-1} A(n(x_{j+1} + sh, t_i)) \text{sign}(sh) \\
&\quad \left. \left. + A(n(x_{j+1+\bar{N}}, t_i)) \text{sign}(\bar{N}h) \right) - n(x_{j-1}, t_i) \left(A(n(x_{j-1-\bar{N}}, t_i)) \right. \right. \\
&\quad \cdot \text{sign}(-\bar{N}h) + 2 \sum_{s=-\bar{N}+1}^{\bar{N}-1} A(n(x_{j-1} + sh, t_i)) \text{sign}(sh) \\
&\quad \left. \left. + A(n(x_{j-1+\bar{N}}, t_i)) \text{sign}(\bar{N}h) \right) \right] \\
&\quad + \mu k \left[n(x_j, t_i) \left(1 - \frac{n(x_j, t_i)}{n_0} \right) \right], \tag{6.5}
\end{aligned}$$

for $i = 1, 2, \dots, M + 1$, and $j = 1, 2, \dots, N + 1$, where $A(n(x + x_0, t)) = n(x + x_0, t)[2 - n(x + x_0, t)]$. In (6.5) near the boundary points, we have assumed that

$$n(x_j, t_i) = n(x_1, t_i) \text{ for } j < 1, \quad \text{and } n(x_j, t_i) = n(x_{N+1}, t_i) \text{ for } j > N + 1.$$

The solution of this numerical scheme is given by a $(N + 1) \times (M + 1)$ matrix. For the stability of this explicit numerical scheme, it is required that the step-length ratio Dk/h^2 is small (for standard linear heat equation, it is well-known that we require $Dk/h^2 < 1/2$).

6.1.2 Numerical results and figures

In order to simulate the traveling wave solutions of (6.1), we first choose the Neumann Boundary Conditions and the following initial function of cell density:

$$n(x, 0) = \begin{cases} 0, & x \in (-l, 0), \\ n_0, & x \in (0, l). \end{cases} \quad (6.6)$$

Using MATLAB, the results of the numerical scheme (6.5) are shown in Figure 6.1, Figure 6.3 and Figure 6.5 by choosing different values of α . The values of other parameters are given by $D = 1$, $n_0 = 1$, and $\mu = 1$. When α is small, the increasing traveling waves exist; see Figure 6.1. However, with the increasing of α , there exists a hump in the wave solution at the beginning of time, which gradually stabilizes to a monotone wavefront in the long term; see Figure 6.3. As α is large enough, the solution still moves with a speed, but there exists an oscillation in the solution shape; see Figure 6.5. The results show a good agreement with the solutions and figures of the non-local models in [34] and [37].

The biological meaning of this situation has a significant relation to the growth of cell population. Specifically, the existence of traveling wave solutions to the cell adhesion model (6.1) implies the rapid growth and expansion from its initial range; see [34] and [37]. This shows an essential effect on the cancer invasion process.

6.1.3 A second numerical approach

Here we should mention the novel numerical approach for (6.1) proposed in [4] and [23], where the main idea was the approximation of the nonlocal integral $S(n(x, t))$ by a local term. We expand the function within the integral as a Taylor series and compare this approximation to a PDE models whose behavior has been previously studied. The

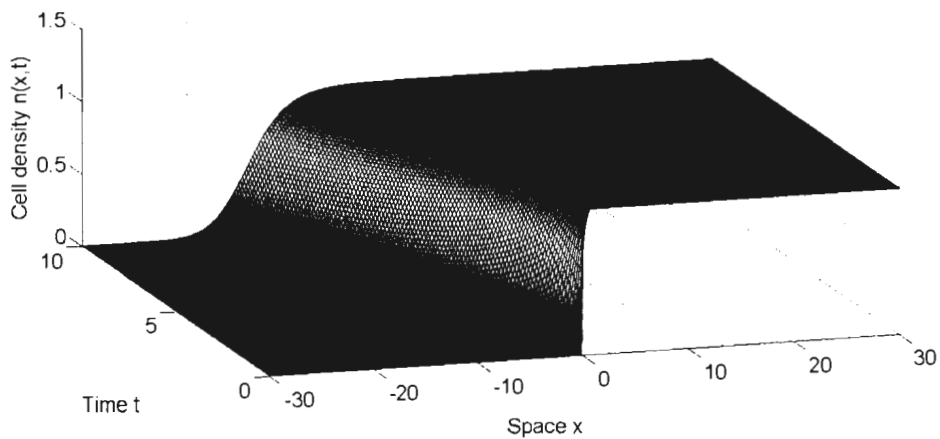


Figure 6.1: Numerical solutions of the model (6.1) with $\alpha = 0.1$. Traveling wave solutions of cell density $n(x,t)$ for time period $t \in [0, 10]$ with the initial conditions (6.6) and $\alpha = 0.1$.

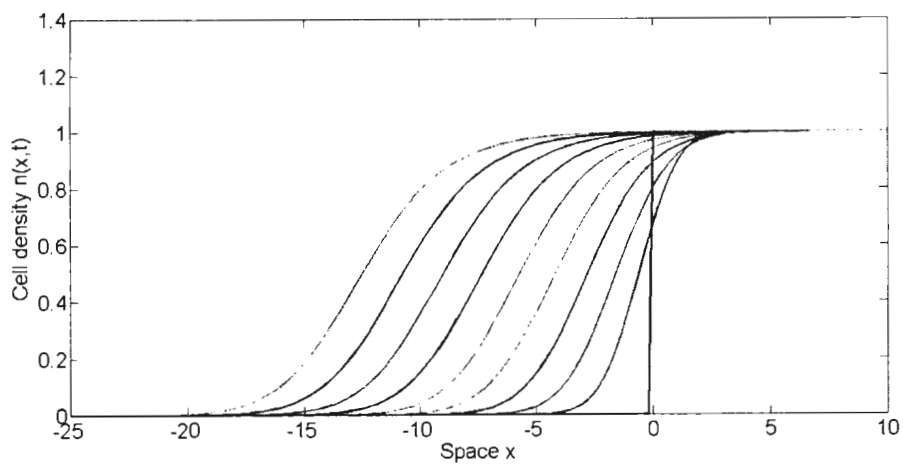


Figure 6.2: Numerical solutions of the model (6.1) with $\alpha = 0.1$. Traveling wave solutions of cell density $n(x,t)$ at different time points for $\alpha = 0.1$.

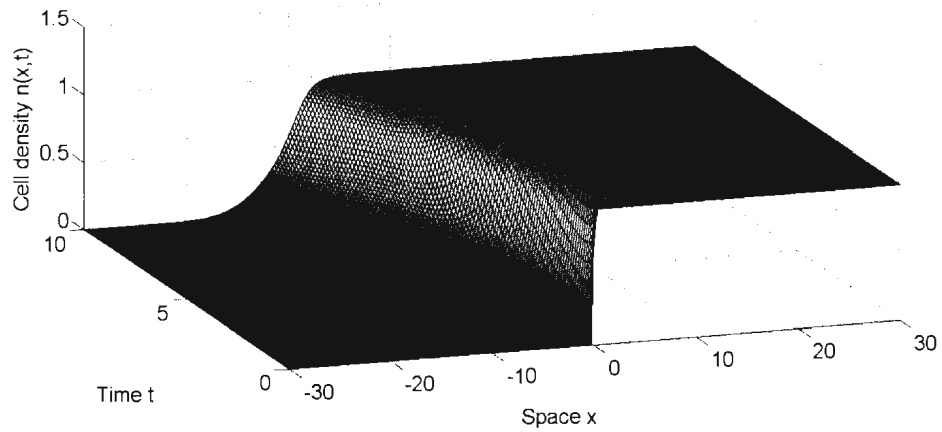


Figure 6.3: Numerical solutions of the model (6.1) with $\alpha = 1$. Traveling wave solutions of cell density $n(x, t)$ for time period $t \in [0, 10]$ with the initial conditions (6.6) and $\alpha = 1$.

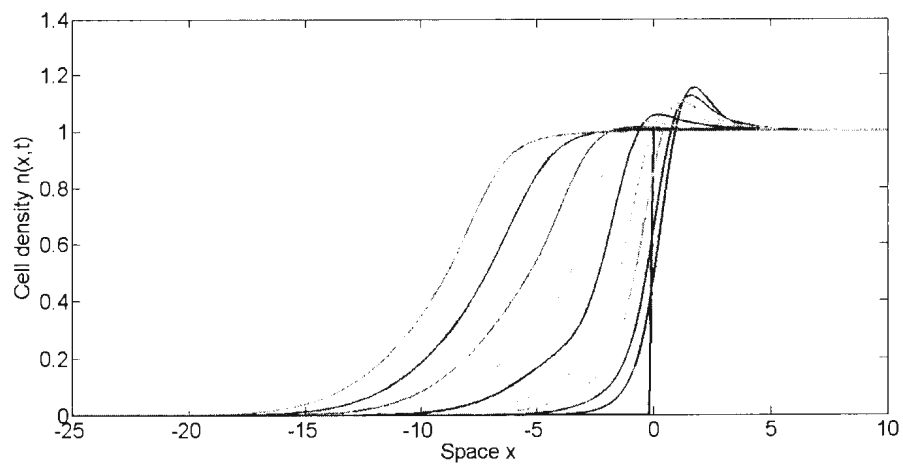


Figure 6.4: Numerical solutions of the model (6.1) with $\alpha = 1$. Traveling wave solutions of cell density $n(x, t)$ at different time points for $\alpha = 1$.

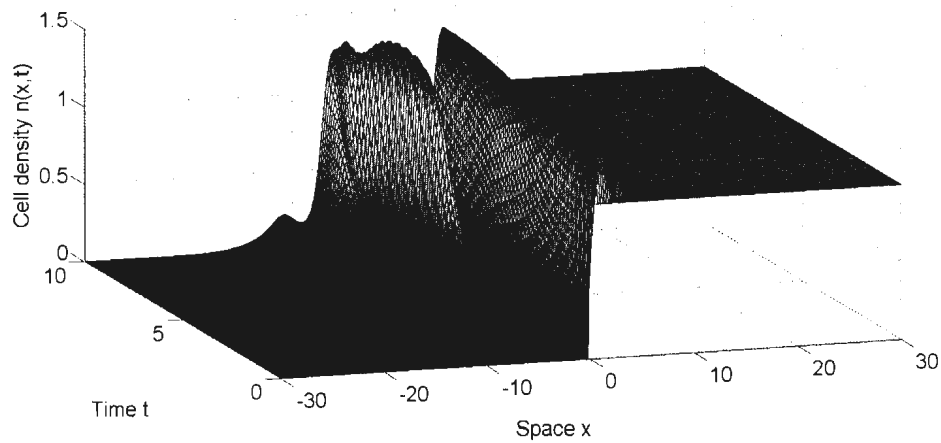


Figure 6.5: Numerical solutions of the model (6.1) with $\alpha = 2$. Traveling wave solutions of cell density $n(x,t)$ for time period $t \in [0, 10]$ with the initial conditions (6.6) and $\alpha = 2$.

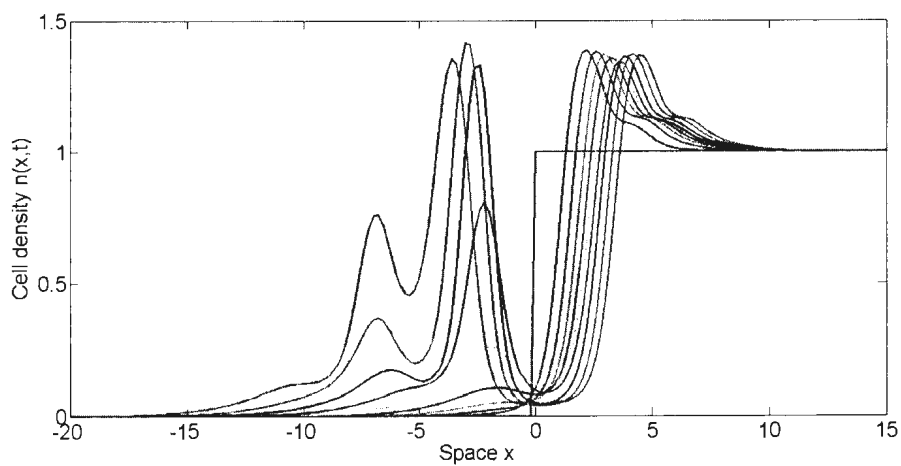


Figure 6.6: Numerical solutions of the model (6.1) with $\alpha = 2$. Traveling wave solutions of cell density $n(x,t)$ at different time points for $\alpha = 2$.

numerical scheme follows the method of lines by first using the same discretization of the non-local models in space and yielding an initial value problem for a large system of ordinary differential equations. Similarly, we use a central differencing scheme for diffusion and adhesion terms and solve the equation numerically by using ODE15s in MATLAB. See [4] and [26] for details.

We start by providing a different difference formula of (6.1) at location x_j given by

$$\begin{aligned}
n_t(x_j, t) &= D \frac{\partial^2 n(x_j, t)}{\partial x_j^2} - \frac{\partial}{\partial x_j} [n(x_j, t) S(n(x_j, t))] + \mu \left[n(x_j, t) \left(1 - \frac{n(x_j, t)}{n_0} \right) \right] \\
&= D \frac{\partial^2 n(x_j, t)}{\partial x_j^2} - \left[\frac{\partial n(x_j, t)}{\partial x_j} S(n(x_j, t)) + \frac{\partial S(n(x_j, t))}{\partial x_j} n(x_j, t) \right] \\
&\quad + \mu \left[n(x_j, t) \left(1 - \frac{n(x_j, t)}{n_0} \right) \right] \\
&= D \frac{n(x_{j+1}, t) - 2n(x_j, t) + n(x_{j-1}, t)}{h^2} - \left[\frac{n(x_{j+1}, t) - n(x_{j-1}, t)}{2h} S(n(x_j, t)) \right. \\
&\quad \left. + n(x_j, t) \frac{S(n(x_{j+1}, t)) - S(n(x_{j-1}, t))}{2h} \right] \\
&\quad + \mu \left[n(x_j, t) \left(1 - \frac{n(x_j, t)}{n_0} \right) \right], \tag{6.7}
\end{aligned}$$

where $j = 1, 2, 3, \dots, N + 1$.

6.1.3.1 Approximation of $S(n(x, t))$

To approximate the integral $S(n(x, t))$, one expands the local adhesive forces $A(n(x + x_0, t))$ within this integral at x as a Taylor series and obtains

$$A(n(x + x_0, t)) = \sum_{s=0}^r \frac{x_0^s}{s!} \frac{\partial^s}{\partial x^s} A(n(x, t)) + O(x_0^{r+1}), \tag{6.8}$$

where r is an even integer. Multiplying (6.8) by $\alpha \text{sign}(x_0)$, and integrating it over the interval $[-1, 1]$ gives

$$\begin{aligned}
S(n(x, t)) &= \alpha \int_{-1}^1 A(n(x + x_0, t)) \text{sign}(x_0) dx_0 \\
&\approx \alpha \int_{-1}^1 \left(\sum_{s=0}^r \frac{x_0^s}{s!} \frac{\partial^s}{\partial x^s} A(n(x, t)) \right) \text{sign}(x_0) dx_0 \\
&= \alpha \int_{-1}^1 A(n(x, t)) \text{sign}(x_0) dx_0 + \alpha \int_{-1}^1 x_0 \frac{\partial A(n(x, t))}{\partial x} \text{sign}(x_0) dx_0 \\
&\quad + \alpha \int_{-1}^1 \frac{x_0^2}{2!} \frac{\partial^2 A(n(x, t))}{\partial x^2} \text{sign}(x_0) dx_0 + \alpha \int_{-1}^1 \frac{x_0^3}{3!} \frac{\partial^3 A(n(x, t))}{\partial x^3} \text{sign}(x_0) dx_0 \\
&\quad + \dots .
\end{aligned} \tag{6.9}$$

Since $\omega(x_0)$ is an odd function, the terms with odd order derivatives in (6.9) disappear, which implies that

$$\begin{aligned}
S(n(x, t)) &= 2\alpha \sum_{s=0}^{\frac{r}{2}-1} \frac{\partial^{2s+1}}{\partial x^{2s+1}} A(n(x, t)) \int_0^1 \frac{x_0^{2s+1}}{(2s+1)!} dx_0 \\
&= 2\alpha \sum_{s=0}^{\frac{r}{2}-1} \frac{1}{(2s+2)!} \frac{\partial^{2s+1}}{\partial x^{2s+1}} A(n(x, t)) \\
&= \alpha \frac{\partial A(n(x, t))}{\partial x} + \frac{\alpha}{12} \frac{\partial^3 A(n(x, t))}{\partial x^3} + \dots .
\end{aligned} \tag{6.10}$$

Neglecting the higher order terms in (6.10), we have the following approximation:

$$S(n(x, t)) = \alpha \frac{\partial A(n(x, t))}{\partial x} = 2\alpha(1-n)n_x. \tag{6.11}$$

$S(n(x_j, t_i))$ in (6.2) is therefore given by applying the central difference method as follows:

$$S(n(x_j, t_i)) = 2\alpha(1 - n(x_j, t_i)) \frac{n(x_{j+1}, t_i) - n(x_{j-1}, t_i)}{2h}. \quad (6.12)$$

6.1.3.2 Numerical results

Substituting (6.12) into (6.7), the numerical scheme of (6.1) is given by

$$\begin{aligned} n_t(x_j, t) = & D \frac{n_{j+1} - 2n_j + n_{j-1}}{h^2} - \frac{\alpha}{2h^2} [(1 - n_j)(n_{j+1} - n_{j-1})^2] \\ & - \frac{\alpha}{2h^2} [n_j(1 - n_{j+1})(n_{j+2} - n_j)] - \frac{\alpha}{2h^2} [n_j(1 - n_{j-1})(n_j - n_{j-2})] \\ & + \mu \left[n_j \left(1 - \frac{n_j}{n_0} \right) \right]. \end{aligned} \quad (6.13)$$

By using the same initial function (6.6) of the cell density and Neumann boundary conditions, the results of this numerical simulation show a good agreement with the ones mentioned. However, comparing to scheme (6.5), when α is large, we observe that this method cannot give a good numerical approximation, since only one term in (6.10) is taken; see Figures 6.7 and 6.8.

6.2 Traveling waves of the cancer invasion model for small χ

In this section, we present the computational simulations of traveling wave solutions to the non-local cancer invasion model (4.4) with both cell-cell and cell-matrix adhesion for relatively small χ . Considering the condition required for $g(\xi)$ in chapter 4, we

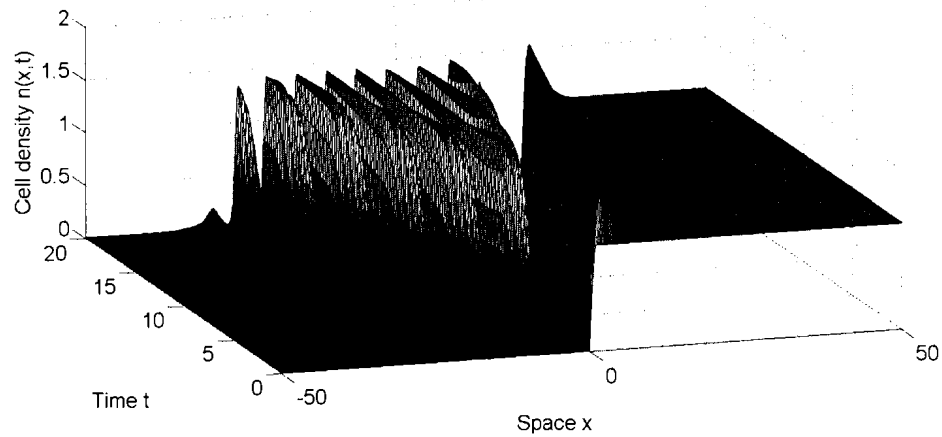


Figure 6.7: Numerical solutions of the model (6.1) with $\alpha = 3$. Traveling wave solutions of cell density $n(x,t)$ for time period $t \in [0, 20]$ with the initial conditions (6.6) and $\alpha = 3$.

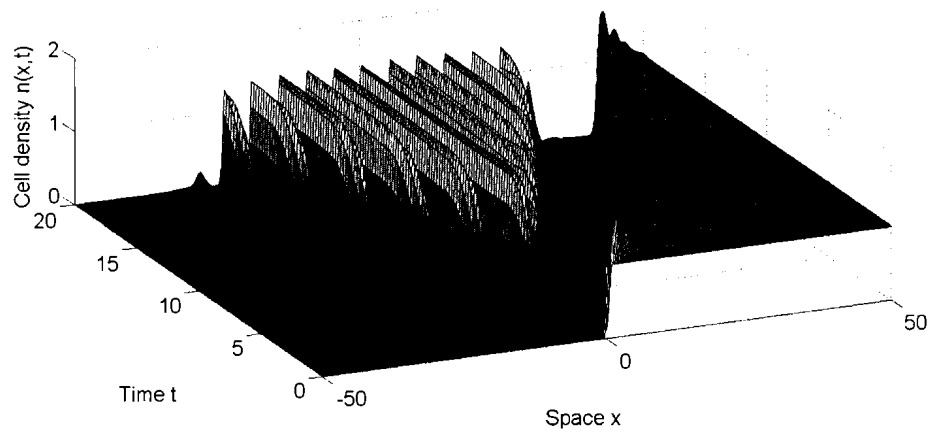


Figure 6.8: Numerical solutions of the model (6.1) with $\alpha = 5$. Traveling wave solutions of cell density $n(x,t)$ for time period $t \in [0, 20]$ with the initial conditions (6.6) and $\alpha = 5$.

know that $0 < n + m < 2$, and it follows that

$$g(n(x + x_0, t) + m(x + x_0, t)) = 2 - n(x + x_0, t) - m(x + x_0, t).$$

Hence the non-local reaction-diffusion model (4.4) for cancer invasion is given by

$$\begin{cases} \frac{\partial n(x,t)}{\partial t} = D \frac{\partial^2 n(x,t)}{\partial x^2} - \frac{\partial}{\partial x} [n(x,t)K(n(x,t), m(x,t))] + \mu n \left(1 - \frac{n}{n_0}\right), \\ \frac{\partial m(x,t)}{\partial t} = -\gamma n m^2, \end{cases} \quad (6.14)$$

where

$$\begin{aligned} K(n(x,t), m(x,t)) &= \chi \int_{-1}^1 \bar{A}(n(x + x_0, t), m(x + x_0, t)) \omega(x_0) dx_0 \\ &= \chi \int_{-1}^1 (\alpha n + \beta m)(2 - n - m) \text{sign}(x_0) dx_0. \end{aligned} \quad (6.15)$$

6.2.1 The finite difference scheme of the cancer invasion model

In this simulation, we approximate the tumor cell density $n(x, t)$ and the extracellular matrix density $m(x, t)$ by using the similar finite difference method as in section 6.1,

that is, the numerical scheme of system (6.14) at location x_j and time t_i is given by

$$\begin{aligned}
\frac{n(x_j, t_{i+1}) - n(x_j, t_i)}{k} &= D \frac{\partial^2 n(x_j, t_i)}{\partial x_j^2} - \frac{\partial}{\partial x_j} \left[n(x_j, t_i) K(n(x_j, t_i), m(x_j, t_i)) \right] \\
&\quad + \mu \left[n(x_j, t_i) \left(1 - \frac{n(x_j, t_i)}{n_0} \right) \right] \\
&= D \frac{n(x_{j+1}, t_i) - 2n(x_j, t_i) + n(x_{j-1}, t_i)}{h^2} \\
&\quad - \frac{1}{2h} \left[n(x_{j+1}, t_i) K(n(x_{j+1}, t_i), m(x_{j+1}, t_i)) \right. \\
&\quad \left. - n(x_{j-1}, t_i) K(n(x_{j-1}, t_i), m(x_{j-1}, t_i)) \right] \\
&\quad + \mu \left[n(x_j, t_i) \left(1 - \frac{n(x_j, t_i)}{n_0} \right) \right], \\
\frac{m(x_j, t_{i+1}) - m(x_j, t_i)}{k} &= -\gamma n(x_j, t_i) m^2(x_j, t_i), \tag{6.16}
\end{aligned}$$

where

$$K(n(x_j, t_i), m(x_j, t_i)) = \chi \int_{-1}^1 \bar{A}(n(x_j + x_0, t_i), m(x_j + x_0, t_i)) \omega(x_0) dx_0. \tag{6.17}$$

To apply the Composite Trapezoidal rule, we discretize the space length x_0 by using the same step size h of x and choose $2\bar{N}$ intervals symmetrically around x_j . Then the

integral $K(n(x_j, t_i), m(x_j, t_i))$ is written as a sum given by

$$\begin{aligned}
K(n(x_j, t_i), m(x_j, t_i)) \approx & \frac{\chi h}{2} \left[\bar{A}(n(x_{j-\bar{N}}, t_i), m(x_{j-\bar{N}}, t_i)) \text{sign}(-\bar{N}h) \right. \\
& + 2 \sum_{s=-\bar{N}+1}^{\bar{N}-1} \bar{A}(n(x_j + sh, t_i), m(x_j + sh, t_i)) \text{sign}(sh) \\
& \left. + \bar{A}(n(x_{j+\bar{N}}, t_i), m(x_{j+\bar{N}}, t_i)) \text{sign}(\bar{N}h) \right]. \quad (6.18)
\end{aligned}$$

6.2.2 Numerical figures and results

The initial condition of tumor cell density $n(x, t)$ is the same as in section 6.1:

$$n(x, 0) = \begin{cases} 0, & x \in (-l, 0), \\ n_0, & x \in (0, l), \end{cases} \quad (6.19)$$

and the smooth initial matrix distribution $m(x, t)$ is given by

$$m(x, 0) = \frac{1}{2} + \frac{1}{2} \tanh(-0.1x), \quad x \in (-l, l). \quad (6.20)$$

The simulation results are shown in Figures 6.9 - 6.20, where we choose the same parameters $D = 1$, $n_0 = 1$, $\gamma = 1$ and $\mu = 1$. For the invasion growth of tumor cells, we let $\alpha = 1$ and $\beta = 2$ ($\alpha < \beta$). When $\chi = 1$ that is relatively small, it presents smooth traveling waves for both tumor cell density and extracellular matrix density, and the wavefronts appear to be strictly monotone. See Figures 6.9 and 6.10. The wavefronts of $n(x, t)$ and $m(x, t)$ at different time points during $t \in [0, 10]$ are shown by Figures 6.11 and 6.12, respectively. Increasing the adhesion coefficient to $\chi = 6$, gives Figures 6.13 and 6.14, where the wave speed increases. There exists a small hump in the wavefronts of $n(x, t)$ at the beginning of time (Figures 6.15 and 6.16).

However, the resulting fronts finally stabilize to a smooth monotone wavefront in the long term. For sufficiently large χ , we show the results by setting $\chi = 25$; see Figures 6.17 and 6.18. A big oscillation appears in the waves of $n(x, t)$ for $t \in [0, 1]$; see Figure 6.19. Eventually the solution $n(x, t)$ of system (6.14) stabilizes to 1 and $m(x, t)$ to 0 (Figures 6.19 and 6.20). The results show a good agreement with the solutions and figures of the non-local models in [34] and [37].

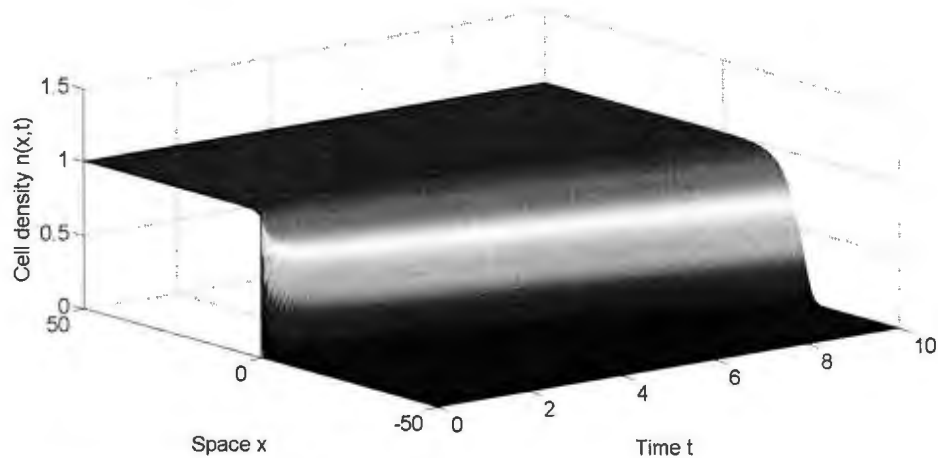


Figure 6.9: Numerical solutions of system (6.14) for $\chi = 1$. Traveling wave solutions of the tumor cell density $n(x, t)$.

6.2.3 A second numerical approach

Considering the method used in [4] and [23], we can also provide an alternate approach to solve system (6.14) numerically. We start by providing a different difference formula

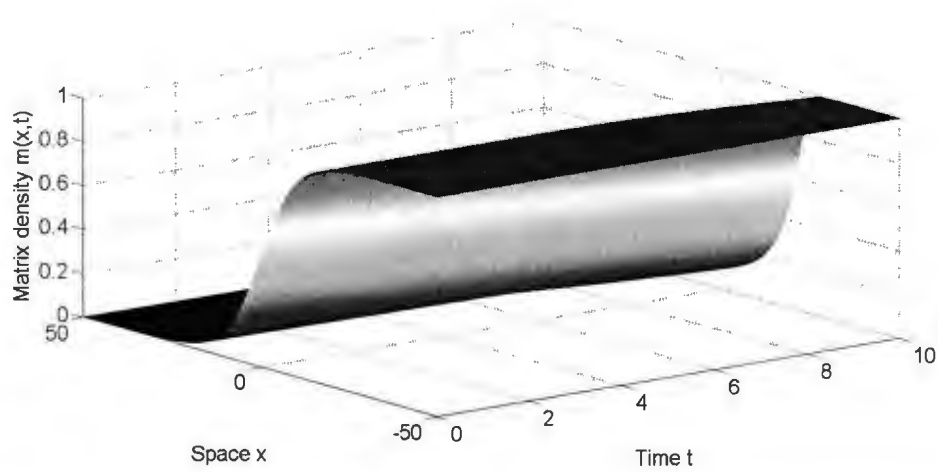


Figure 6.10: Numerical solutions of system (6.14) for $\chi = 1$. Traveling wave solutions of the extracellular matrix density $m(x,t)$.

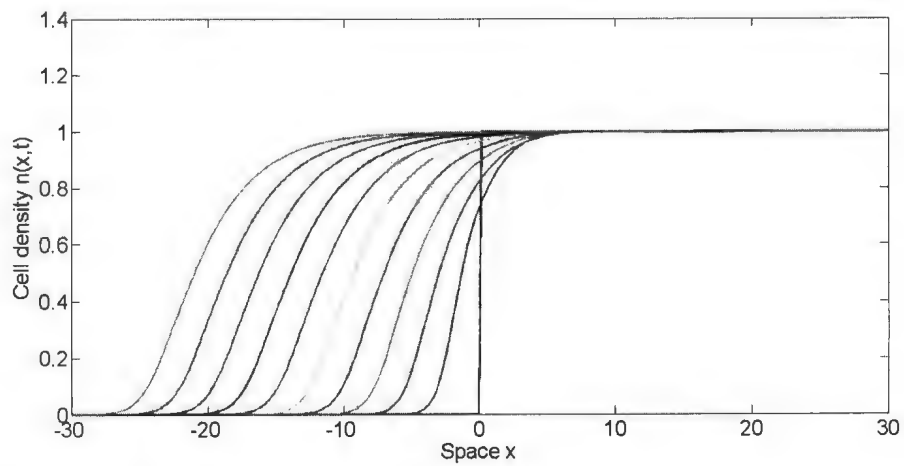


Figure 6.11: Numerical solutions of system (6.14) for $\chi = 1$. Wavefronts of the tumor cell density $n(x,t)$ at different time points for $t \in [0, 10]$.

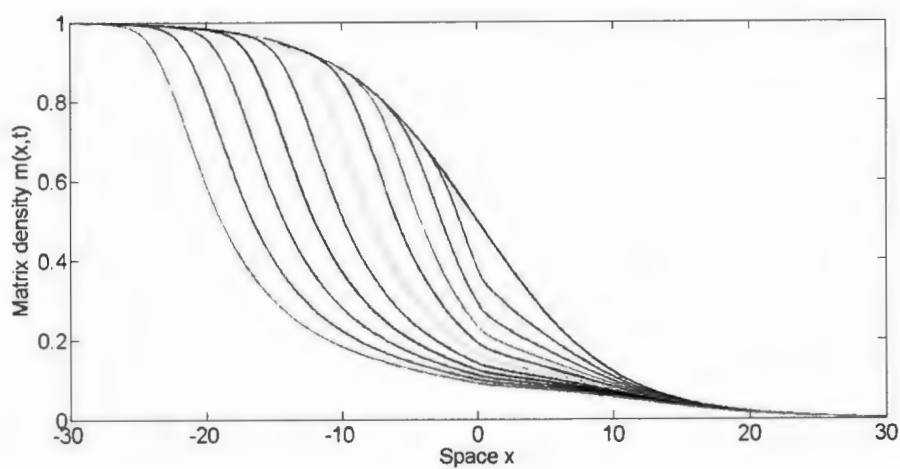


Figure 6.12: Numerical solutions of system (6.14) for $\chi = 1$. Wavefronts of the extracellular matrix density $m(x, t)$ at different time points for $t \in [0, 10]$.

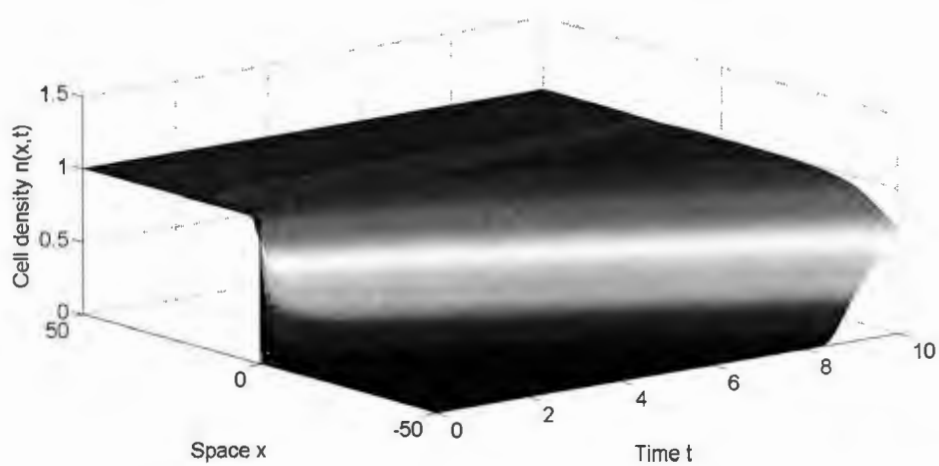


Figure 6.13: Numerical solutions of system (6.14) for $\chi = 6$. Traveling wave solutions of the tumor cell density $n(x, t)$.

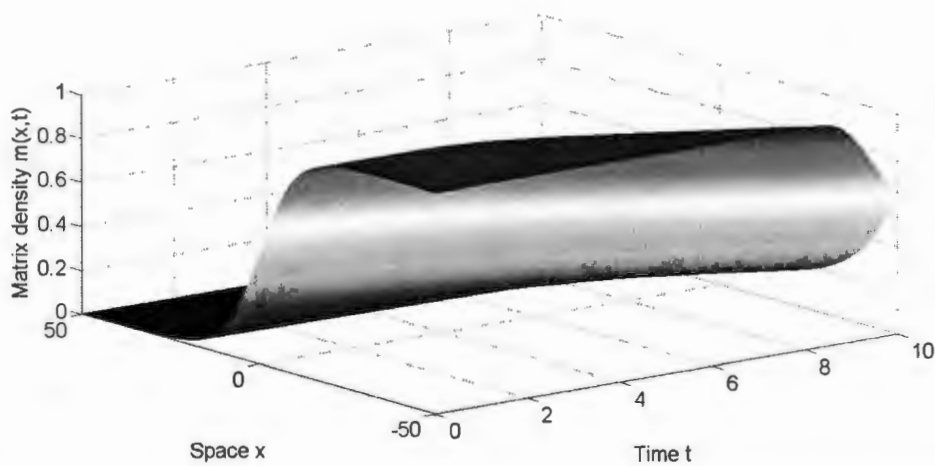


Figure 6.14: Numerical solutions of system (6.14) for $\chi = 6$. Traveling wave solutions of the extracellular matrix density $m(x,t)$.

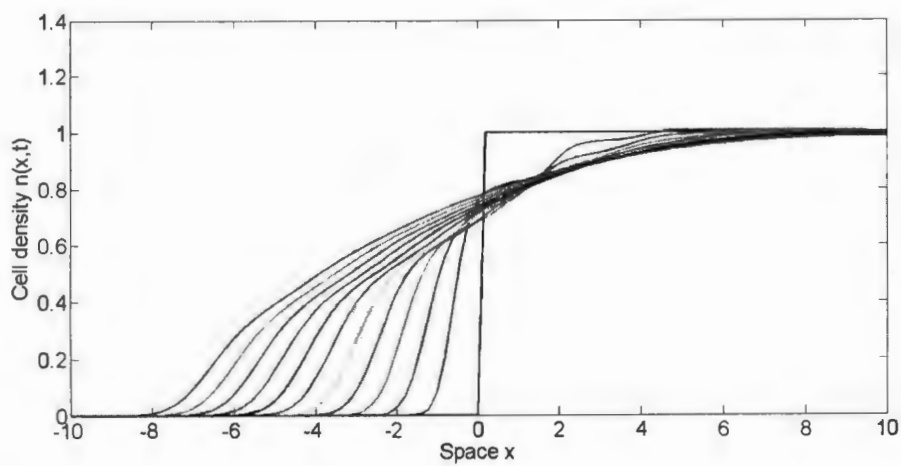


Figure 6.15: Numerical solutions of system (6.14) for $\chi = 6$. Wavefronts of the tumor cell density $n(x,t)$ at different time points in the beginning for $t \in [0, 1]$.

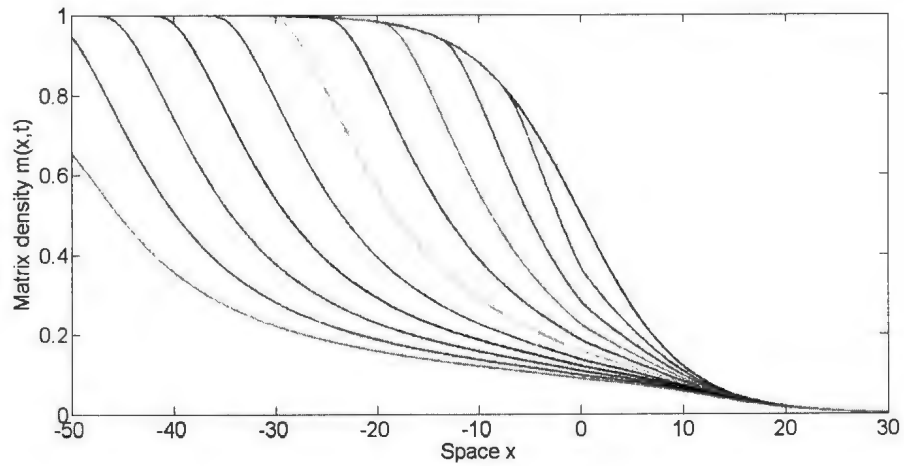


Figure 6.16: Numerical solutions of system (6.14) for $\chi = 6$. Wavefronts of the extracellular matrix density $m(x, t)$ at different time points for $t \in [0, 10]$.

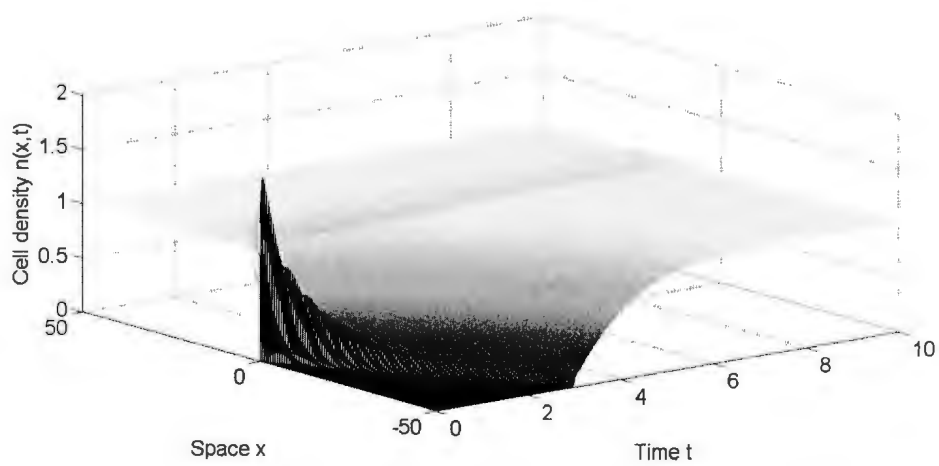


Figure 6.17: Numerical solutions of system (6.14) for $\chi = 25$. Traveling wave solutions of the tumor cell density $n(x, t)$.

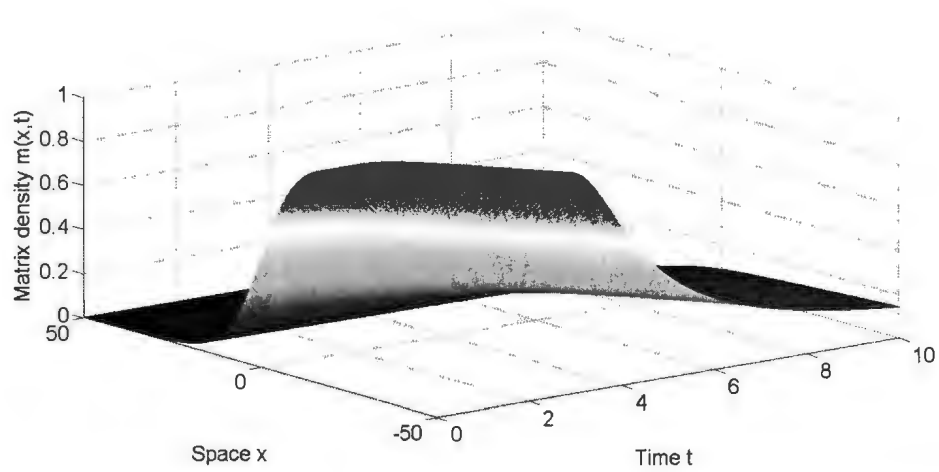


Figure 6.18: Numerical solutions of system (6.14) for $\chi = 25$. Traveling wave solutions of the extracellular matrix density $m(x,t)$.

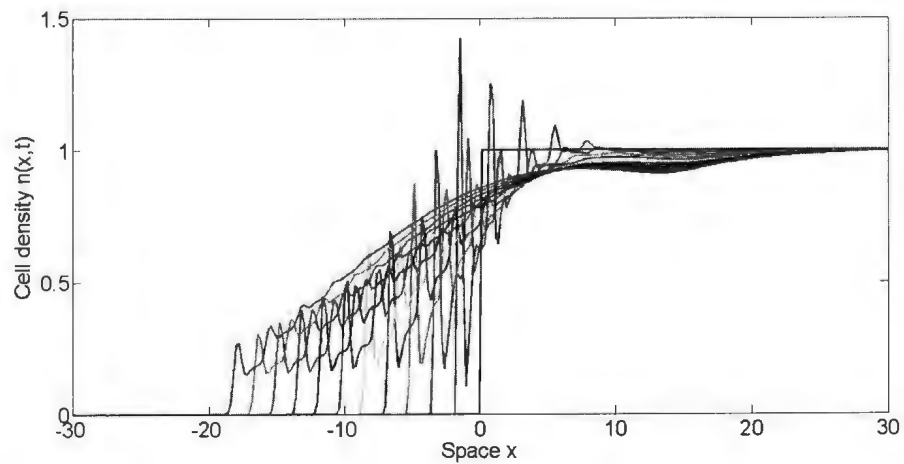


Figure 6.19: Numerical solutions of system (6.14) for $\chi = 25$. Wavefronts of the tumor cell density $n(x,t)$ at different time points in the beginning for $t \in [0, 1]$.

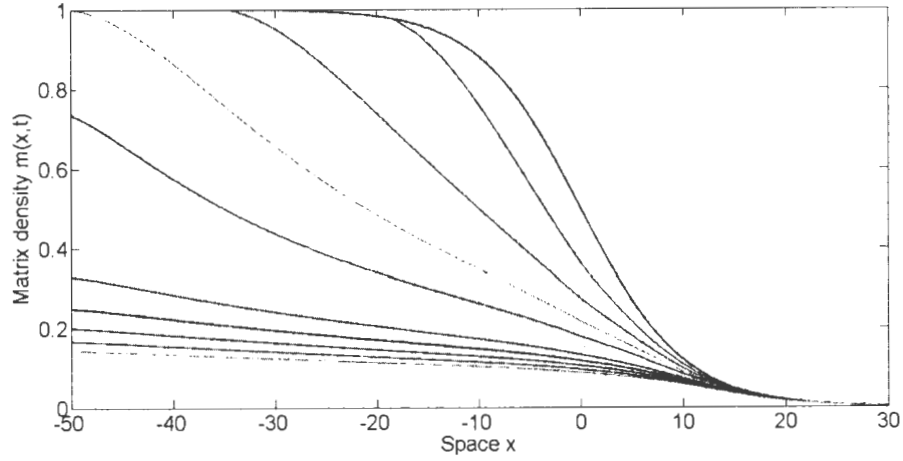


Figure 6.20: Numerical solutions of system (6.14) for $\chi = 25$. Wavefronts of the extracellular matrix density $m(x,t)$ at different time points for $t \in [0, 10]$.

of system (6.14) at location x_j given by

$$\begin{aligned}
 n_t(x_j, t) = & D \frac{n(x_{j+1}, t) - 2n(x_j, t) + n(x_{j-1}, t)}{h^2} \\
 & - \left[\frac{n(x_{j+1}, t) - n(x_{j-1}, t)}{2h} K(n(x_j, t), m(x_j, t)) \right. \\
 & \left. + n(x_j, t) \frac{K(n(x_{j+1}, t), m(x_{j+1}, t)) - K(n(x_{j-1}, t), m(x_{j-1}, t))}{2h} \right] \\
 & + \mu \left[n(x_j, t) \left(1 - \frac{n(x_j, t)}{n_0} \right) \right], \\
 m_t(x_j, t) = & -\gamma n(x_j, t) m^2(x_j, t). \tag{6.21}
 \end{aligned}$$

6.2.3.1 Approximation of $K(n(x, t), m(x, t))$

Using the same method as in section 6.1, we expand $\bar{A}(n(x+x_0, t), m(x+x_0, t))$ within this integral at x as a Taylor series:

$$\bar{A}(n(x+x_0, t), m(x+x_0, t)) = \sum_{s=0}^r \frac{x_0^s}{s!} \frac{\partial^s}{\partial x^s} \bar{A}(n(x, t), m(x, t)) + O(x_0^{r+1}), \quad (6.22)$$

where r is an even integer. Multiplying (6.22) by $\chi \text{sign}(x_0)$ and then integrating over the interval $[-1, 1]$, we obtain the following approximation of $K(n(x, t), m(x, t))$:

$$\begin{aligned} K(n(x, t), m(x, t)) &= \chi \int_{-1}^1 \bar{A}(n(x+x_0, t), m(x+x_0, t)) \omega(x_0) dx_0 \\ &\approx 2\chi \sum_{s=0}^{\frac{r}{2}-1} \frac{1}{(2s+2)!} \frac{\partial^{2s+1}}{\partial x^{2s+1}} \bar{A}(n(x, t), m(x, t)) \\ &= \chi \frac{\partial \bar{A}(n(x, t), m(x, t))}{\partial x} + O(x_0^3) \\ &\approx \chi(\alpha n_x + \beta m_x)(2 - n - m) \\ &\quad - \chi(\alpha n + \beta m)(n_x + m_x). \end{aligned} \quad (6.23)$$

Applying the central difference scheme for the first-order derivatives, $K(n(x_j, t), m(x_j, t))$ in (6.21) is therefore given by

$$\begin{aligned} K(n(x_j, t), m(x_j, t)) &= -\chi(\alpha n_j + \beta m_j) \left(\frac{n_{j+1} - n_{j-1}}{2h} + \frac{m_{j+1} - m_{j-1}}{2h} \right) \\ &\quad + \chi \left(\alpha \frac{n_{j+1} - n_{j-1}}{2h} + \beta \frac{m_{j+1} - m_{j-1}}{2h} \right) \\ &\quad \cdot (2 - n_j - m_j), \end{aligned} \quad (6.24)$$

where $n_j = n(x_j, t)$ and $m_j = m(x_j, t)$ are the densities at time t location x_j of the tumor cells and extracellular matrix, respectively.

6.2.3.2 Numerical results

This numerical scheme is eventually given by a direct substitution of (6.24) into (6.21). By using the same initial functions (6.19) and (6.20) as above and the Neumann boundary conditions for both densities, the results of this numerical simulation show a good agreement with the ones mentioned. However, comparing to scheme (6.16), when χ is large, we observe that this method cannot give a good numerical approximation, since only one term in (6.23) is taken. Applying this numerical scheme, it is evident that humps appear when the adhesion coefficient χ is relatively small. In Figure 6.21, there exists a hump in the wavefront of $n(x, t)$ at the beginning of the time for $\chi = 7$; see also Figure 6.22.

6.2.4 An alternate initial function for matrix distribution

In the above subsection, we choose the step initial function for the tumor cell density and the smooth tangent hyperbolic function for the extracellular matrix density in order to investigate a traveling wave solution for system (6.14). However, the choice of the initial function can be adjustable as long as it is given by connecting the limits of the waves. In [34], the authors considered a cosine function for the matrix density $m(x, t)$. In this subsection, we simulate system (6.14) by applying the same step function for $n(x, 0)$ and a sine function for the initial condition $m(x, 0)$ given as follows:

$$m(x, 0) = \frac{1}{2} - \frac{1}{2} \sin\left(\frac{\pi}{2l}x\right), \quad x \in (-l, l). \quad (6.25)$$

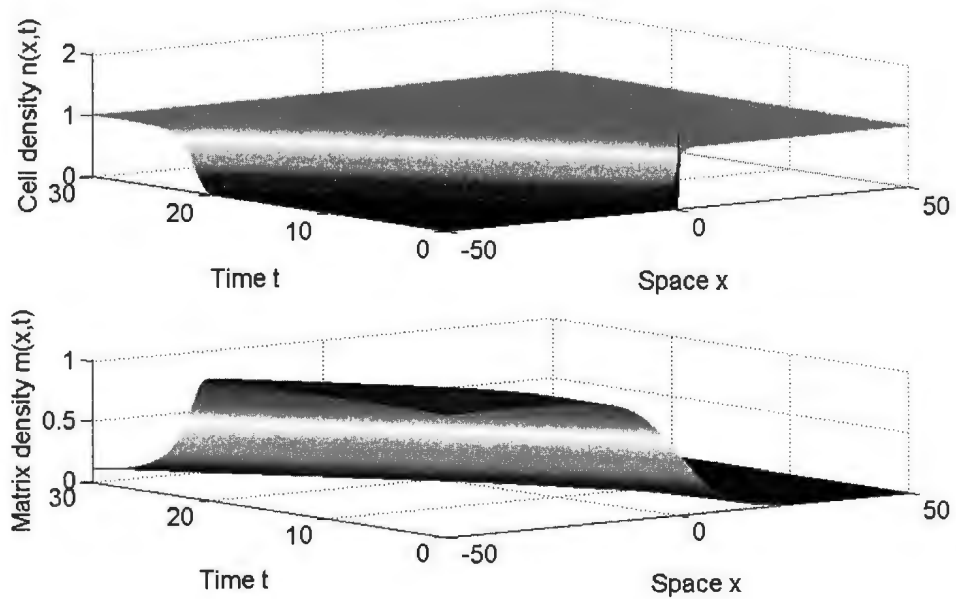


Figure 6.21: Numerical solutions of system (6.14) for $\chi = 7$. These are the solution figures of tumor cell density $n(x, t)$ (upper wave) and extracellular matrix density $m(x, t)$ (lower wave) for time period $t \in [0, 30]$ with the adhesion coefficient $\chi = 7$.

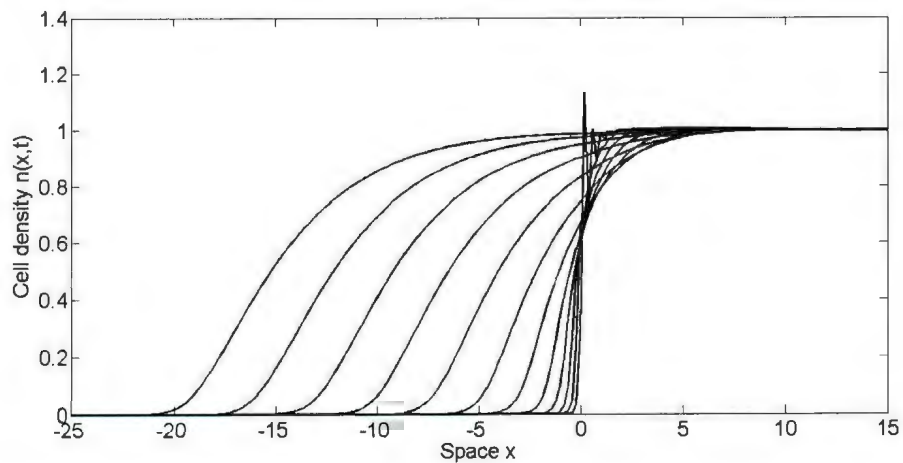


Figure 6.22: Numerical solutions of system (6.14) for $\chi = 7$. Wavefronts of the tumor cell density $n(x, t)$ at different time points.

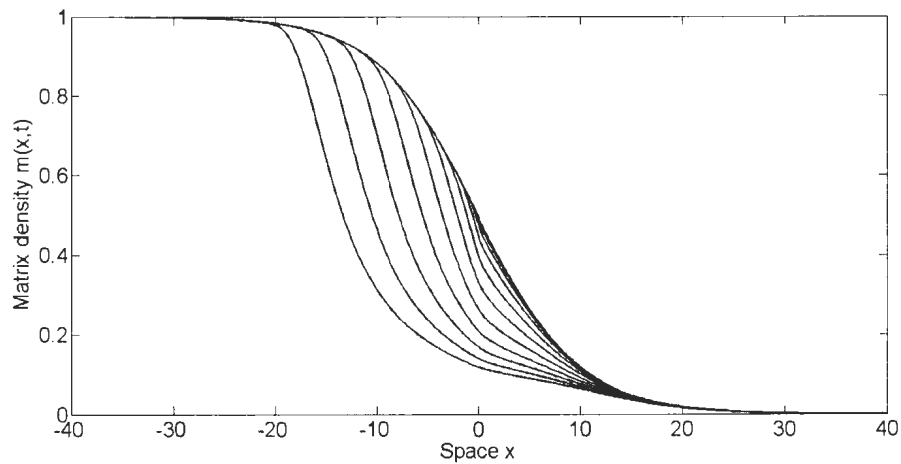


Figure 6.23: Numerical solutions of system (6.14) for $\chi = 7$. Wavefronts of the extracellular matrix density $m(x,t)$ at different time points.

By using the scheme in section 6.2.4, the results are shown in Figures 6.24 - 6.32. When $\chi = 1$ is small, it presents smooth waves in Figure 6.24 for both cell and matrix densities. See also Figures 6.25 and 6.26 for an interpretation of the changing process. Increasing χ leads the appearance of a hump at the beginning of time; see figures 6.27 and 6.30. Furthermore, the larger value of χ leads to the larger hump. The results show a good agreement with the ones in the above section. See also Figures 6.28, 6.29, 6.31 and 6.32 for more details.

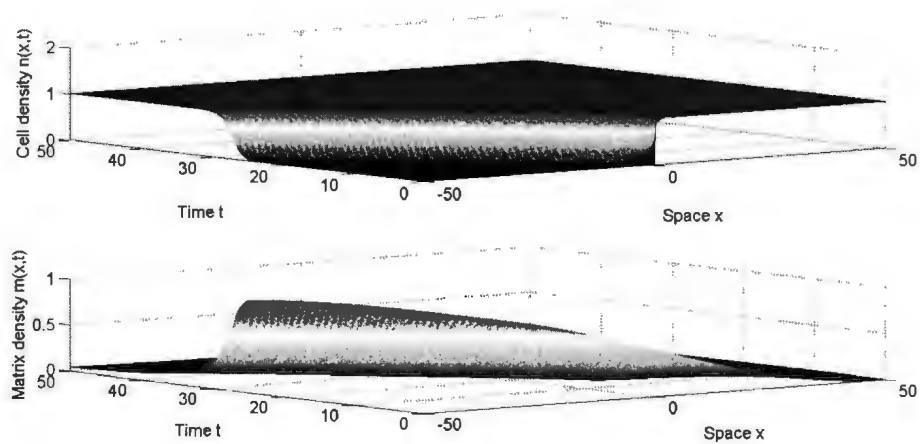


Figure 6.24: Numerical solutions of system (6.14) for $\chi = 1$. These are the solution figures of tumor cell density $n(x, t)$ (upper wave) and extracellular matrix density $m(x, t)$ (lower wave) with the adhesion coefficient $\chi = 1$.

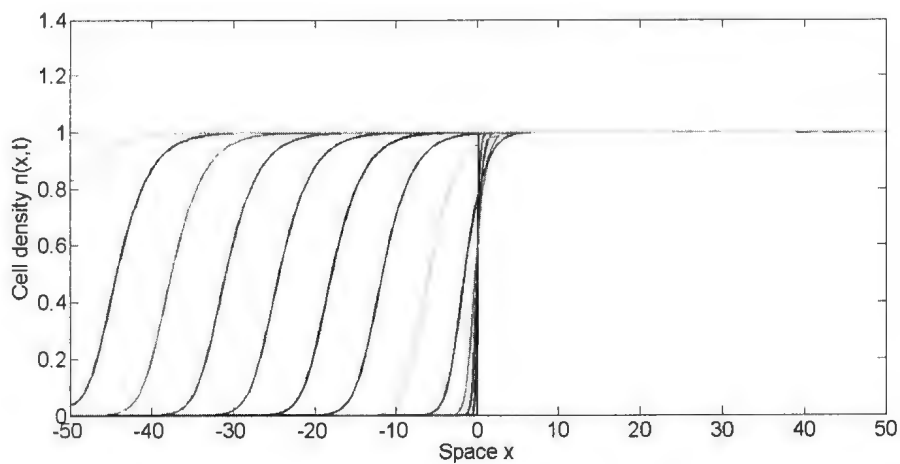


Figure 6.25: Numerical solutions of system (6.14) for $\chi = 1$. Wavefronts of the tumor cell density $n(x, t)$ at different time points.

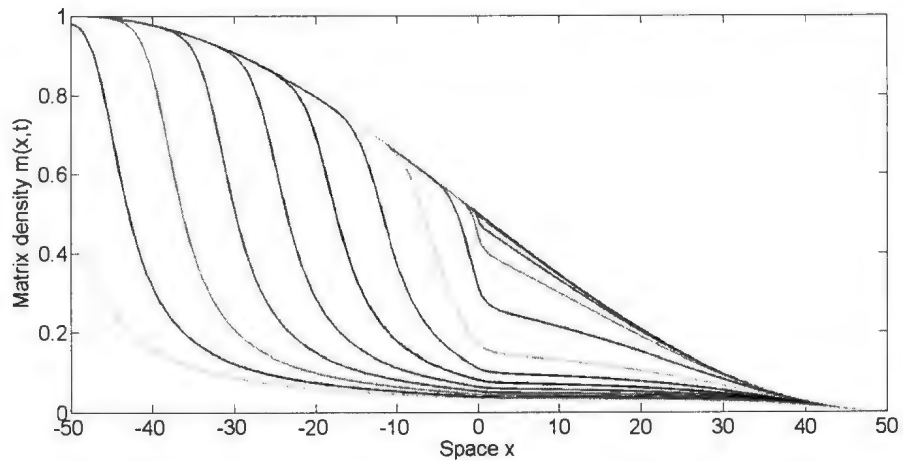


Figure 6.26: Numerical solutions of system (6.14) for $\chi = 1$. Wavefronts of the extracellular matrix density $m(x, t)$ at different time points.

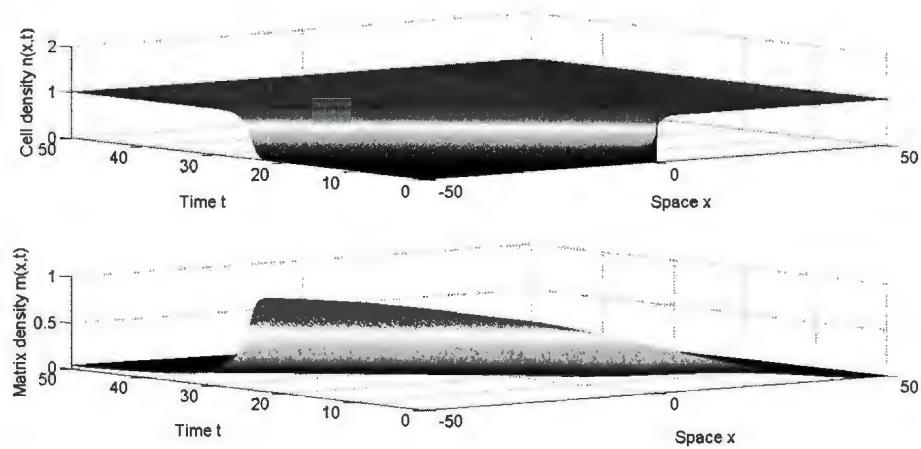


Figure 6.27: Numerical solutions of system (6.14) for $\chi = 4$. These are the solution figures of tumor cell density $n(x, t)$ (upper wave) and extracellular matrix density $m(x, t)$ (lower wave) with the adhesion coefficient $\chi = 4$.

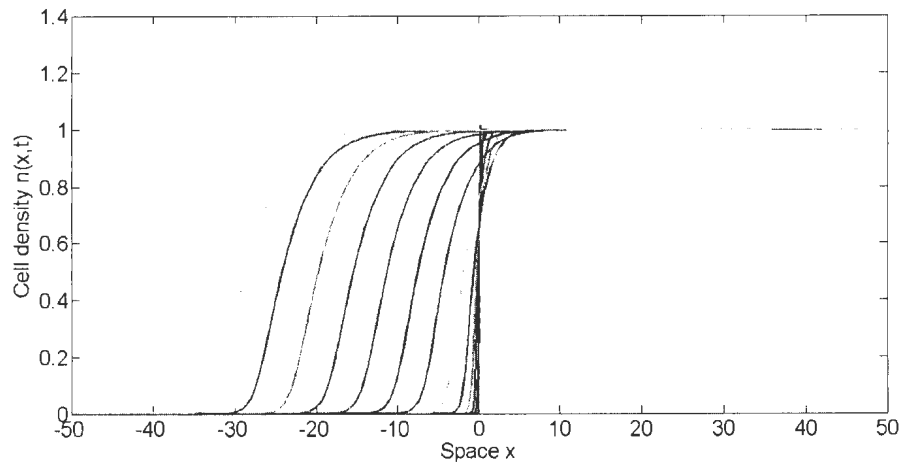


Figure 6.28: Numerical solutions of system (6.14) for $\chi = 4$. Wavefronts of the tumor cell density $n(x, t)$ at different time points.

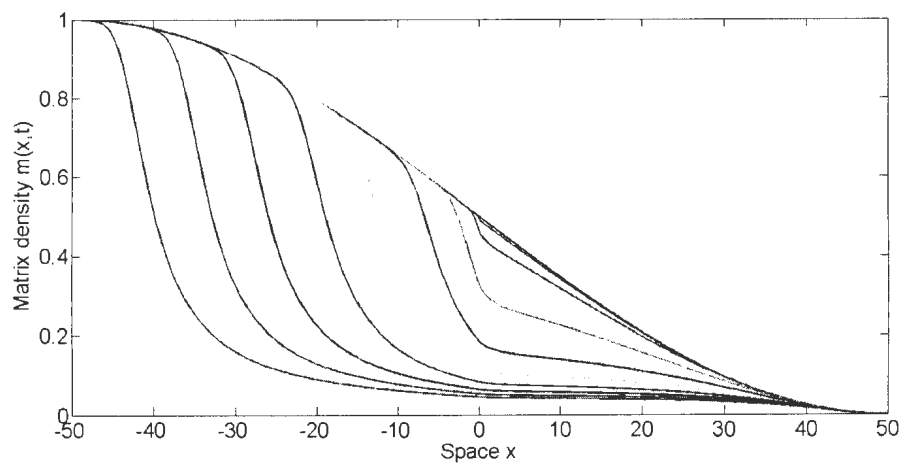


Figure 6.29: Numerical solutions of system (6.14) for $\chi = 4$. Wavefronts of the extracellular matrix density $m(x, t)$ at different time points.

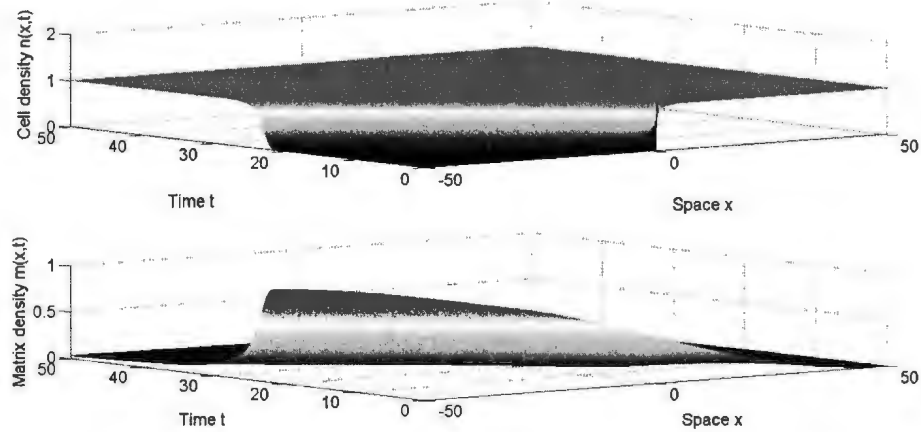


Figure 6.30: Numerical solutions of system (6.14) for $\chi = 6$. These are the solution figures of tumor cell density $n(x, t)$ (upper wave) and extracellular matrix density $m(x, t)$ (lower wave) with the adhesion coefficient $\chi = 6$.

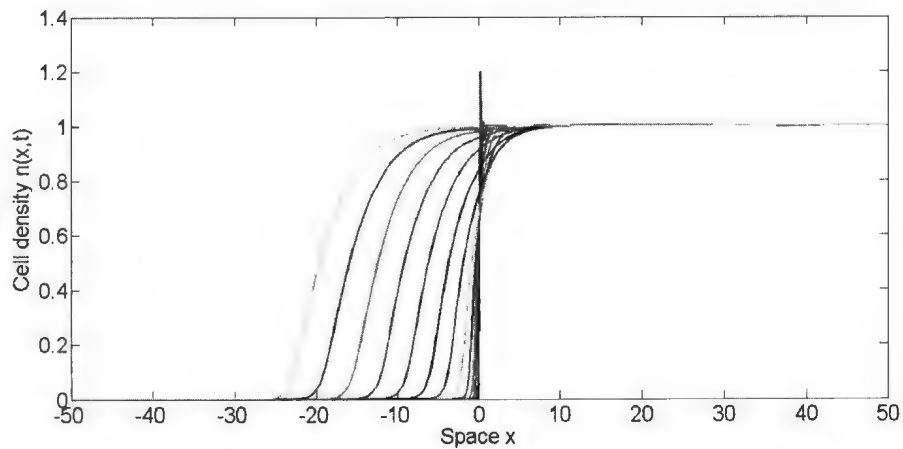


Figure 6.31: Numerical solutions of system (6.14) for $\chi = 6$. Wavefronts of the tumor cell density $n(x, t)$ at different time points.

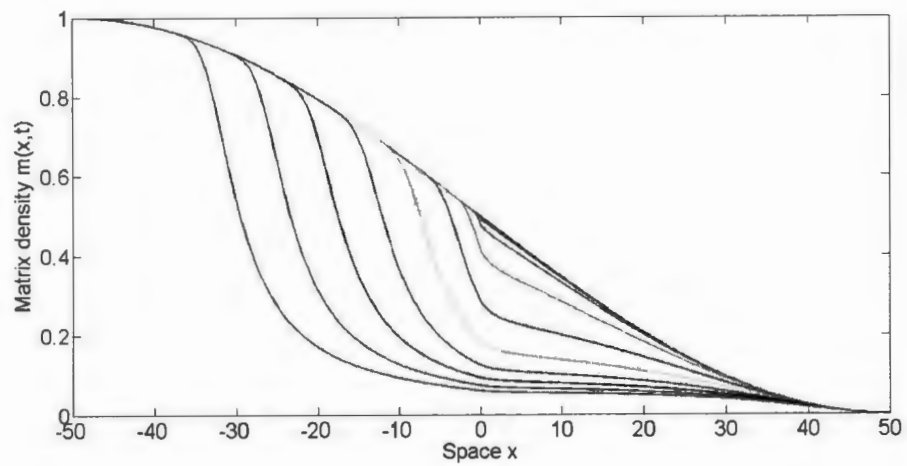


Figure 6.32: Numerical solutions of system (6.14) for $\chi = 6$. Wavefronts of the extracellular matrix density $m(x, t)$ at different time points.

Chapter 7

Discussion

Previously, Armstrong *et al.* [4] and Sherratt *et al.* [37] developed a continuum model for cell adhesion by approximating the non-local term in a PDE, and they also demonstrated the cell aggregation patterns in numerical simulations. To investigate the requirement of cell-matrix adhesion to dominate cell-cell adhesion in an invasive phenotype, Sherratt *et al.* [37] extended to propose a new model for cancer invasion. The invasive growth of tumor cell was given numerically in both 1D and 2D by Painter *et al.* [34]. In this paper, we first apply the perturbation methods and Banach fixed point theorem, and prove the existence of traveling wave solutions to the above non-local model of cell adhesion with the relatively small adhesion coefficient α . We also demonstrate the similar result for the cancer invasion model, where the traveling wave solutions exist when the adhesion coefficient χ is relatively small. Numerical simulations are conducted to confirm our theoretical results. The Composite Trapezoidal rule is used to approximate the integral of the non-local term in the PDE model. The results of 2D invasion model has been provided numerically by Painter *et al.* [34], in which it shows exactly an existence of traveling waves. Some theoretical work is needed to explore the 2D cases for both cell adhesion and cancer invasion

models. Furthermore, the oscillations that appeared in section 6 for both models with sufficiently large adhesion coefficients also deserve our further study in the future.

Bibliography

- [1] A. R. A. Anderson, *A hybrid mathematical model of solid tumour invasion: the importance of cell adhesion*, IMA J. Math. Appl. Med. Biol., 22 (2005), pp. 163-186.
- [2] A. R. A. Anderson, M. A. J. Chaplain, E. L. Newman, R. J. C. Steele and A. M. Thompson, *Mathematical modelling of tumour invasion and metastasis*, Comput. Math. Methods Med., 2 (2000), pp. 129-154.
- [3] R. Araujo and L. McElwain, *A history of the study of solid tumour growth: The contribution of mathematical modelling*, Bull. Math. Biol., 66 (2004), pp. 1039-1091.
- [4] N. J. Armstrong, K. J. Painter and J. A. Sherratt, *A continuum approach to modelling cell-cell adhesion*, J. Theor. Biol., 243 (2006), pp. 98-113.
- [5] H. M. Byrne and M. A. J. Chaplain, *Modelling the role of cell-cell adhesion in the growth and development of carcinomas*, Math. Comp. Modelling, 24 (1996), pp. 1-17.
- [6] M. A. J. Chaplain and G. Lolas, *Mathematical modelling of cancer cell invasion of tissue: the role of the urokinase plasminogen activation system*, Math. Models Methods Appl. Sci., 15 (2005), pp. 1685-1734.

- [7] M. A. J. Chaplain and G. Lolas, *Mathematical modelling of cancer invasion of tissue: dynamic heterogeneity*, *Net. Hetero. Med.*, 1 (2006), pp. 399-439.
- [8] M. A. J. Chaplain, *Avascular growth, angiogenesis and vascular growth in solid tumours: the mathematical modelling of the stages of tumour development*, *Math. Comp. Modelling*, 23 (1996), pp. 47-87.
- [9] V. Cristini, J. Lowengrub and Q. Nic, *Nonlinear simulation of tumour growth*, *Math. Biol.*, 46 (2003), pp. 191-224.
- [10] S. Dorman and A. Deutsch, *Modelling of self organized avascular tumour growth with a hybrid automaton*, *In Silico Biology*, 2 (2002), pp. 1-35.
- [11] D. Drasdo and S. Holme, *A single-cell-based model of tumour growth in vitro: Monolayers and spheroids*, *Phys. Biol.*, 2 (2005), pp. 133-147.
- [12] T. Faria, W. Huang and J. Wu, *Traveling waves for delayed reaction-diffusion equations with global response*, *Proc. R. Soc. Lond. Ser. A Math. Phys. Eng. Sci.*, 462 (2006), pp. 229-261.
- [13] J. Folkman, *Tumor angiogenesis*, *Adv. Cancer Res.*, 19 (1974), pp. 331-358.
- [14] J. Folkman, *The vascularization of tumors*, *Sci. Am.*, 234 (1976), pp. 58-73.
- [15] J. Folkman and M. Klagsbrun, *Angiogenic factors*, *Science*, 235 (1987), pp. 442-447.
- [16] R. A. Foty and M. S. Steinberg, *The differential adhesion hypothesis: a direct evaluation*, *Dev. Biol.*, 278 (2005), pp. 255-263.
- [17] H. B. Frieboes, X. Zheng, C. H. Sun, B. Tromberg, R. Gatenby and V. Cristini, *An integrated computational/experimental model of tumor invasion*, *Cancer Res.*, 66 (2006), pp. 1597-1604.

- [18] H. B. Frieboes, J. S. Lowengrub, S. Wise, X. Zheng, P. Macklin, E. L. Bearer and V. Cristini, *computer simulation of glioma growth and morphology*, Neuroimage, 37 (2007), pp. 59-70.
- [19] A. Friedman, *Mathematical analysis and challenges arising from models of tumor growth*, Math. Mod. Meth. Appl. Sci., 17 (2007), pp. 1751-1772.
- [20] P. Gassmann, A. Enns and J. Haier, *Role of tumor cell adhesion and migration in organ-specific metastasis formation*, Onkologic, 27 (2004), pp. 577-582.
- [21] R. A. Gatenby, *Models of tumor-host interaction as competing populations: implications for tumor biology and treatment*, J. Theor. Biol., 176 (1995), pp. 447-455.
- [22] R. A. Gatenby and E. T. Gawlinski, *A reaction-diffusion model of cancer invasion*, Cancer Res., 56 (1996), pp. 5745-5753.
- [23] A. Gerischi and M. A. J. Chaplain, *Mathematical modelling of cancer cell invasion of tissue: Local and non-local models and the effect of adhesion*, J. Theor. Biol., 250 (2008), pp. 684-704.
- [24] J. M. Halbleib and W. J. Nelson, *Cadherins in development: cell adhesion, sorting, and tissue morphogenesis*, Genes Dev., 20 (2006), pp. 3199-3214.
- [25] I. Hart, *The spread of tumors*. In: M. Knowles and P. Selby (editors), *Introduction to the cellular and molecular biology of cancer*, Oxford University Press, Oxford, UK, 2005, pp. 447-455.
- [26] T. Hillen, K. Painter and C. Schmeiser, *Global existence for chemotaxis with finite sampling radius*, AIMS DCDS-B, 7 (2007), pp. 125-144.

- [27] Ignacio Ramis-Conde, M. A. J. Chaplain and A. R. A. Anderson, *Mathematical modelling of cancer cell incasion of tissue*, Math. Comp. Modelling, 47 (2008), pp. 533-545.
- [28] J. Jeon, V. Quaranta and P. T. Cummings, *An off-lattice hybrid discrete-continuum model of tumor growth and invasion*, Biophysical J., 98 (2010), pp. 37-47.
- [29] P. Macklin and J. Lowengrub, *Nonlinear simulation of the effect of microenvironment on tumor growth*, J. Theor. Biol., 245 (2007), pp. 677-704.
- [30] K. Mischaikow, H. Smith and H. R. Thieme, *Asymptotically autonomous semiflows: chain recurrence and Lyapunov functions*, Trans. Amer. Math. Soc., 347 (1995), pp. 1669-1685.
- [31] J.D. Murray, *Mathematical Biology. I and II*, Springer-Verlag, New York, 2002.
- [32] C. Ou and J. Wu, *Traveling wavefronts in a delayed food-limited population model*, SIAM J. Math. Anal., 39 (2007), pp. 103-125.
- [33] C. Ou and W. Yuan, *Traveling wavefronts in a volume-filling chemotaxis model*, SIAM J. Applied Dynamical Systems, 8 (2009), pp. 390-416.
- [34] K. J. Painter, N. J. Armstrong and J. A. Sherratt, *The impact of adhesion on cellular invasion processes in cancer and development*, J. Theor. Biol., 264 (2010), pp. 1057-1067.
- [35] K. J. Palmer, *Exponential dichotomies and transversal homoclinic points*, J. Differ. Equ., 55 (1984), pp. 225-256.
- [36] P. J. Reddig and R. L. Juliano, *Clinging to life: Cell to matrix adhesion and cell survival*, Cancer Metastasis Rev., 24 (2005), pp. 425-439.

- [37] J. A. Sherratt, S. A. Gourley, N. J. Armstrong and K. J. Painter, *Boundedness of solutions of a non-local reaction-diffusion model for adhesion in cell aggregation and cancer invasion*, European J. Appl. Math., 20 (2009), pp. 123-144.
- [38] S. Turner and J. A. Sherratt, *Intercellular adhesion and cancer invasion: A discrete simulation using the extended Potts model*, J. Theor. Biol., 216 (2002), pp. 85-100.
- [39] P. Zigrino, S. Loffek and C. Mauch, *Tumor-stroma interactions: their role in the control of tumor cell invasion*, Biochemic, 87 (2005), pp. 321-328.

